

ENERGY STABILITY AND ERROR ESTIMATES OF EXPONENTIAL TIME DIFFERENCING SCHEMES FOR THE EPITAXIAL GROWTH MODEL WITHOUT SLOPE SELECTION

LILI JU, XIAO LI, ZHONGHUA QIAO, AND HUI ZHANG

ABSTRACT. In this paper, we propose a class of exponential time differencing (ETD) schemes for solving the epitaxial growth model without slope selection. A linear convex splitting is first applied to the energy functional of the model, and then Fourier collocation and ETD-based multistep approximations are used respectively for spatial discretization and time integration of the corresponding gradient flow equation. Energy stabilities and error estimates of the first and second order ETD schemes are rigorously established in the fully discrete sense. We also numerically demonstrate the accuracy of the proposed schemes and simulate the coarsening dynamics with small diffusion coefficients. The results show the logarithm law for the energy decay and the power laws for growth of the surface roughness and the mound width, which are consistent with the existing theories in the literature.

1. INTRODUCTION

Let us consider the two-dimensional model of epitaxial thin film growth without slope selection taking on the form [11]

$$(1.1) \quad \frac{\partial u}{\partial t} = -\nabla \cdot \left(\frac{\nabla u}{1 + |\nabla u|^2} \right) - \varepsilon^2 \Delta^2 u, \quad \mathbf{x} \in \Omega, \quad t \in (0, T],$$

where $\Omega = (x_0, x_0 + X) \times (y_0, y_0 + Y)$ is a rectangular domain, $\varepsilon > 0$ is a constant parameter, and $u = u(\mathbf{x}, t)$ is the scaled height function of the thin film subject to the periodic boundary condition. This model (1.1) describes the coarsening processes arising from many applications in physics, chemistry and biology [25], in

Received by the editor June 10, 2016, and, in revised form, November 7, 2016, and January 4, 2017.

2010 *Mathematics Subject Classification.* Primary 35Q99, 47A56, 65M12, 65M70.

Key words and phrases. Thin film growth, exponential time differencing, Fourier collocation, linear convex splitting, energy stability, error estimates.

The first author's research was partially supported by the US National Science Foundation grant DMS-1521965.

The second author's research was partially supported by the Hong Kong Research Grant Council GRF grant 15302214 during his visit at the Hong Kong Polytechnic University and China Postdoctoral Science Foundation grant 2017M610748.

The third author is the corresponding author. The third author's research was partially supported by the Hong Kong Research Grant Council GRF grant 15302214, NSFC/RGC Joint Research Scheme N_HKBU204/12 and the Hong Kong Polytechnic University internal grant 1-ZE33.

The fourth author's research was partially supported by NSFC/RGC Joint Research Scheme 11261160486, NSFC grants 11471046, 11571045 and the Ministry of Education Program for New Century Excellent Talents Project NCET-12-0053.

which the nonlinear second order term models the Ehrlich-Schwoebel effect and the linear fourth order term the surface diffusion. The equation is mass conservative along the time evolution due to

$$(1.2) \quad \int_{\Omega} u(\mathbf{x}, t) \, d\mathbf{x} = \int_{\Omega} u(\mathbf{x}, 0) \, d\mathbf{x}, \quad t > 0,$$

under the periodic boundary condition.

The equation (1.1) in fact defines a gradient flow with respect to the $L^2(\Omega)$ inner product of the energy functional

$$(1.3) \quad E(u) = \int_{\Omega} \left(-\frac{1}{2} \ln(1 + |\nabla u|^2) + \frac{\varepsilon^2}{2} |\Delta u|^2 \right) \, d\mathbf{x}.$$

The logarithmic term $-\frac{1}{2} \ln(1 + |\mathbf{y}|^2)$, $\mathbf{y} \in \mathbb{R}^2$, is bounded above by zero but unbounded below. Moreover, it has no relative minima, which implies that there are no energetically favored values for $|\nabla u|$. From a physical point of view, it means that there is no slope selection mechanism in the epitaxial growth dynamics. Some detailed discussions on this issue could be found in [17, 18] and the references cited therein. The well-posedness of the initial boundary-value problem involving the equation (1.1) was studied in [17] using the perturbation analysis method.

The physically interesting process is the coarsening dynamics occurring on a very long time scale for spatially large systems, i.e., small ε . For instance, Li and Liu [18] have proved that the energy is bounded below by $\mathcal{O}(-\ln t)$ for large time t and the global minimum energy scales as $\mathcal{O}(\ln \varepsilon)$ in the limit $\varepsilon \rightarrow 0$. Therefore, numerical simulations for the coarsening dynamics of large systems require the long time stability and accuracy of the numerical methods. In particular, temporally and spatially high order schemes with unconditional stability are highly demanded in terms of efficiency and effectiveness.

Energy stability has been investigated recently for numerical schemes of the thin film growth models [23, 24] and other phase field models [6, 10]. Wang et al. [30] derived first order (in time) convex splitting schemes for epitaxial growth models under the convex splitting framework exploited by Eyre [9], and Shen et al. [27] constructed second order (in time) schemes based on the same convex splitting approach. A linear iteration algorithm was further developed for the second order energy stable scheme for the model (1.1) in [3]. We note that these numerical schemes are nonlinear although unconditionally energy stable. A linear convex splitting scheme was developed for the model (1.1) by Chen et al. [2], and their main contribution lies in an alternate convex splitting of the Ehrlich-Schwoebel part in (1.3). The convex splitting technique also has been used extensively on different phase field models, e.g., the Cahn-Hilliard equations [20, 33], the phase field crystal model [31], the diffuse interface model with the Peng-Robinson equation of state [21], etc. On the other hand, second order nonlinear and linearized Crank-Nicolson type difference schemes were derived by Qiao et al. [22] for the model (1.1) where the unconditional energy stability is achieved with respect to a modified energy functional by introducing an auxiliary variable. For the epitaxial growth model with slope selection, Xu and Tang [32] proposed a first order linear implicit-explicit scheme by adding an order $\mathcal{O}(\Delta t)$ stabilization term of the form $A\Delta(u^{n+1} - u^n)$, where A depends nonlinearly on the numerical solutions. In other words, it implicitly uses the L^∞ -bound assumption on $|\nabla u^n|$ in order to make A a controllable constant. In a recent work [19], these technical restrictions were removed and a

more reasonable stability theory was established. The linear scheme presented in [2] was essentially a first order stabilized implicit-explicit scheme with the stabilizer equal to one. Similar approaches were also applied on the Allen-Cahn and Cahn-Hilliard equations [28]. Overall, there exist very few works devoted to development of temporally high order schemes with unconditional energy stability for the model (1.1).

In this paper, we will present fully discrete numerical schemes for solving the model (1.1), that uses the Fourier spectral collocation approximation for spatial discretization in combination with exponential time differencing (ETD) [1, 4, 16] and explicit multistep approximations for time integration. These schemes can be efficiently implemented via the fast Fourier transform (FFT). The ETD-based schemes often involve exact integration of the linear part of the target equation followed by an explicit approximation of the temporal integral of the nonlinear term, and can achieve high accuracy, stability and preservation of the exponential behavior of the system. Hochbruck and Ostermann provided in [13] a nice review on the exponential integrator based methods, including the ETD ones. Du and Zhu investigated the linear stabilities of some ETD schemes [7] and modified ETD schemes [8]. Ju et al. developed stable and compact ETD schemes and their fast implementations for semi-linear second and fourth order parabolic equations [14, 15, 34] by utilizing suitable linear splitting techniques. However, apart from numerical implementations, theoretical analysis on stability and convergence of the ETD schemes for the phase field models are still highly desired.

The rest of the paper is organized as follows. In Section 2, we first present a linear convex splitting of the energy functional (1.3), and then based on this splitting develop a class of fully discrete ETD numerical schemes, in which Fourier spectral collocation is used for spatial discretization and explicit multistep approximations for time integration. The energy stabilities of the first and second order (in time) ETD schemes are proved in Section 3, followed by error estimates rigorously derived in Section 4. In Section 5, we numerically demonstrate the temporal and spatial accuracy of the proposed ETD schemes and simulate the coarsening dynamics with small ε to verify the scaling laws obtained at the theoretical level. Some concluding remarks are given in Section 6.

2. FULLY DISCRETE EXPONENTIAL TIME DIFFERENCING SCHEMES

It is well known [7] that a suitable linear operator splitting can improve the stability. Motivated partly by the work of [2], in this section we first provide a sufficient and necessary condition, independent on the unknown solution u , on the existence of a linear convex splitting of the energy functional (1.3). Then, we discretize the spatial domain and the time interval, respectively, to design fully discrete ETD numerical schemes for (1.3).

2.1. Linear convex splitting. We try to find a linear convex splitting of the energy (1.3) as $E(u) = E_c(u) - E_e(u)$ with

$$(2.1) \quad E_c(u) = \int_{\Omega} \left(\frac{\kappa}{2} |\nabla u|^2 + \frac{\varepsilon^2}{2} |\Delta u|^2 \right) dx, \quad E_e(u) = \int_{\Omega} \left(\frac{\kappa}{2} |\nabla u|^2 + \frac{1}{2} \ln(1 + |\nabla u|^2) \right) dx,$$

where $\kappa > 0$ is expected to be as small as possible. $E_c(u)$ is obviously convex as long as $\kappa > 0$, but the convexity of $E_e(u)$ depends on the convexity of the function

$$G(a, b) = \frac{\kappa}{2}(a^2 + b^2) + \frac{1}{2} \ln(1 + a^2 + b^2), \quad a, b \in \mathbb{R}.$$

Proposition 2.1. *The function $G(a, b)$ is convex in \mathbb{R}^2 if and only if $\kappa \geq \frac{1}{8}$.*

Proof. Simple calculations give us the Hessian matrix

$$\nabla^2 G(a, b) = \frac{1}{(1 + a^2 + b^2)^2} \begin{pmatrix} d_{11}(a^2, b^2) & -2ab \\ -2ab & d_{22}(a^2, b^2) \end{pmatrix}$$

with

$$\begin{aligned} d_{11}(p, q) &= \kappa(p + q)^2 + (2\kappa - 1)p + (2\kappa + 1)q + \kappa + 1, \\ d_{22}(p, q) &= \kappa(p + q)^2 + (2\kappa + 1)p + (2\kappa - 1)q + \kappa + 1. \end{aligned}$$

The convexity of G is thus equivalent to the positive semi-definiteness of the matrix $\nabla^2 G$, that is,

$$(2.2a) \quad d_{11}(p, q) \geq 0,$$

$$(2.2b) \quad d_{22}(p, q) \geq 0,$$

$$(2.2c) \quad d_{11}(p, q)d_{22}(p, q) - 4pq \geq 0,$$

where $p = a^2$ and $q = b^2$. Next we prove that (2.2) holds for any $p, q \geq 0$ if and only if $\kappa \geq \frac{1}{8}$. We rewrite $d_{11}(p, q)$ as

$$d_{11}(p, q) = \kappa q^2 + (2\kappa p + 2\kappa + 1)q + \kappa p^2 + (2\kappa - 1)p + \kappa + 1.$$

Since $\partial_q d_{11}(p, q) > 0$ for any $\kappa > 0$ and $p, q \geq 0$, the inequality $d_{11}(p, q) \geq 0$ holds for any $p, q \geq 0$ if and only if $d_{11}(p, 0) \geq 0$ for any $p \geq 0$, which is equivalent to

$$\begin{cases} -\frac{2\kappa - 1}{2\kappa} > 0, \\ \Delta(d_{11}) = 1 - 8\kappa \leq 0, \end{cases} \quad \text{or} \quad \begin{cases} -\frac{2\kappa - 1}{2\kappa} \leq 0, \\ d_{11}(0, 0) \geq 0, \end{cases}$$

and then leads to $\kappa \geq \frac{1}{8}$. The analysis for the inequality (2.2b) is similar. We next show that the inequality (2.2c) holds for any $p, q \geq 0$ when $\kappa \geq \frac{1}{8}$. It is not hard to find

$$d_{11}(p, q)d_{22}(p, q) - 4pq = (1 + p + q)[1 + \kappa(1 + p + q)]d_0(p, q)$$

with

$$d_0(p, q) = \kappa p^2 + [2\kappa(1 + q) - 1]p + \kappa(1 + q)^2 - q + 1.$$

If $\kappa \geq \frac{1}{8}$, then $\Delta(d_0) = 1 - 8\kappa \leq 0$, which implies that $d_{11}(p, q)d_{22}(p, q) - 4pq \geq 0$ for any $p, q \geq 0$. □

The above convex splitting of the energy (1.3) motivates us to apply ETD schemes to the split form of the equation (1.1) with a splitting constant $\kappa \geq \frac{1}{8}$. To this end, we rewrite the equation (1.1) as

$$(2.3) \quad \frac{\partial u}{\partial t} = -(\varepsilon^2 \Delta^2 - \kappa \Delta)u - \nabla \cdot \left(\frac{\nabla u}{1 + |\nabla u|^2} \right) - \kappa \Delta u.$$

Usually, larger κ leads to more stable numerical schemes, but larger splitting errors.

2.2. Spectral collocation approximations for spatial discretization. Let N_x and N_y be two even numbers. The $N_x \times N_y$ mesh $\Omega_{\mathcal{N}}$ of the domain Ω is a set of nodes (x_i, y_j) with $x_i = x_0 + ih_x$, $y_j = y_0 + jh_y$, $1 \leq i \leq N_x$, $1 \leq j \leq N_y$, where $h_x = \frac{X}{N_x}$ and $h_y = \frac{Y}{N_y}$ are the uniform mesh sizes in each dimension. All of the two-dimensional periodic grid functions defined on $\Omega_{\mathcal{N}}$ are denoted by $\mathcal{M}^{\mathcal{N}}$. We define the index sets

$$J_{\mathcal{N}} = \{(i, j) \in \mathbb{Z}^2 \mid 1 \leq i \leq N_x, 1 \leq j \leq N_y\},$$

$$\widehat{J}_{\mathcal{N}} = \left\{ (k, l) \in \mathbb{Z}^2 \mid -\frac{N_x}{2} + 1 \leq k \leq \frac{N_x}{2}, -\frac{N_y}{2} + 1 \leq l \leq \frac{N_y}{2} \right\}.$$

For a function $f \in \mathcal{M}^{\mathcal{N}}$, the 2-D discrete Fourier transform $\widehat{f} = Pf$ is defined componentwise [26, 29] by

$$\widehat{f}_{kl} = \frac{1}{N_x N_y} \sum_{(i,j) \in J_{\mathcal{N}}} f_{ij} \exp\left(-i\frac{2k\pi}{X}x_i\right) \exp\left(-i\frac{2l\pi}{Y}y_j\right), \quad (k, l) \in \widehat{J}_{\mathcal{N}}.$$

The function f can be reconstructed via the corresponding inverse transform $f = P^{-1}\widehat{f}$ with components given by

$$f_{ij} = \sum_{(k,l) \in \widehat{J}_{\mathcal{N}}} \widehat{f}_{kl} \exp\left(i\frac{2k\pi}{X}x_i\right) \exp\left(i\frac{2l\pi}{Y}y_j\right), \quad (i, j) \in J_{\mathcal{N}}.$$

Let $\widehat{\mathcal{M}}^{\mathcal{N}} = \{Pf \mid f \in \mathcal{M}^{\mathcal{N}}\}$ and define the operators \widehat{D}_x and \widehat{D}_y on $\widehat{\mathcal{M}}^{\mathcal{N}}$ as

$$(\widehat{D}_x \widehat{f})_{kl} = \left(\frac{2k\pi i}{X}\right) \widehat{f}_{kl}, \quad (\widehat{D}_y \widehat{f})_{kl} = \left(\frac{2l\pi i}{Y}\right) \widehat{f}_{kl}, \quad (k, l) \in \widehat{J}_{\mathcal{N}},$$

then the Fourier spectral approximations to the first and second order partial derivatives can be represented as

$$D_x = P^{-1}\widehat{D}_x P, \quad D_y = P^{-1}\widehat{D}_y P, \quad D_x^2 = P^{-1}\widehat{D}_x^2 P, \quad D_y^2 = P^{-1}\widehat{D}_y^2 P.$$

For any $f, g \in \mathcal{M}^{\mathcal{N}}$, $\mathbf{f} = (f^1, f^2)^T \in \mathcal{M}^{\mathcal{N}} \times \mathcal{M}^{\mathcal{N}}$ and $\mathbf{g} = (g^1, g^2)^T \in \mathcal{M}^{\mathcal{N}} \times \mathcal{M}^{\mathcal{N}}$, the discrete gradient, divergence and Laplace operators are given, respectively, by

$$\nabla_{\mathcal{N}} f = \begin{pmatrix} D_x f \\ D_y f \end{pmatrix}, \quad \nabla_{\mathcal{N}} \cdot \mathbf{f} = D_x f^1 + D_y f^2, \quad \Delta_{\mathcal{N}} f = D_x^2 f + D_y^2 f,$$

and the discrete L^2 inner product $(\cdot, \cdot)_{\mathcal{N}}$ and L^2 norm $\|\cdot\|_{\mathcal{N}}$ by

$$(f, g)_{\mathcal{N}} = h_x h_y \sum_{(i,j) \in J_{\mathcal{N}}} f_{ij} g_{ij}, \quad \|f\|_{\mathcal{N}} = \sqrt{(f, f)_{\mathcal{N}}},$$

$$(\mathbf{f}, \mathbf{g})_{\mathcal{N}} = h_x h_y \sum_{(i,j) \in J_{\mathcal{N}}} (f_{ij}^1 g_{ij}^1 + f_{ij}^2 g_{ij}^2), \quad \|\mathbf{f}\|_{\mathcal{N}} = \sqrt{(\mathbf{f}, \mathbf{f})_{\mathcal{N}}}.$$

It is easy to show the following proposition.

Proposition 2.2. *For any functions $f, g \in \mathcal{M}^{\mathcal{N}}$ and $\mathbf{g} \in \mathcal{M}^{\mathcal{N}} \times \mathcal{M}^{\mathcal{N}}$, we have the discrete integration by parts formulas*

$$(f, \nabla_{\mathcal{N}} \cdot \mathbf{g})_{\mathcal{N}} = -(\nabla_{\mathcal{N}} f, \mathbf{g})_{\mathcal{N}}, \quad (f, \Delta_{\mathcal{N}} g)_{\mathcal{N}} = -(\nabla_{\mathcal{N}} f, \nabla_{\mathcal{N}} g)_{\mathcal{N}} = (\Delta_{\mathcal{N}} f, g)_{\mathcal{N}}.$$

By noticing the property (1.2), without loss of generality, we assume that the mean of u is zero and only consider the zero-mean grid functions coming from the $(N_x N_y - 1)$ -dimensional space

$$\mathcal{M}_0^{\mathcal{N}} = \{v \in \mathcal{M}^{\mathcal{N}} \mid (v, 1)_{\mathcal{N}} = 0\} = \{v \in \mathcal{M}^{\mathcal{N}} \mid \widehat{v}_{00} = 0\}.$$

A function $u \in \mathcal{M}^N$ could always be mapped into \mathcal{M}_0^N by the projection

$$u \mapsto u - \frac{1}{XY}(u, 1)_N.$$

Let Δ_N^0 be the limitation of Δ_N on \mathcal{M}_0^N .

Define $\tilde{L}_N = \varepsilon^2 \Delta_N^2 - \kappa \Delta_N$ and its limitation on \mathcal{M}_0^N , $L_N = \varepsilon^2 (\Delta_N^0)^2 - \kappa \Delta_N^0$. It is obvious from Proposition 2.2 that \tilde{L}_N is symmetric (or self-adjoint) on \mathcal{M}^N , i.e.,

$$(\tilde{L}_N u, v)_N = (u, \tilde{L}_N v)_N, \quad \forall u, v \in \mathcal{M}^N.$$

Moreover, for any $u \in \mathcal{M}_0^N$, we have

$$(L_N u, u)_N = \varepsilon^2 \|\Delta_N u\|_N^2 + \kappa \|\nabla_N u\|_N^2 \geq 0, \quad (L_N u, u)_N = 0 \iff u = 0,$$

which means that the operator L_N is symmetric positive definite (thus invertible) on \mathcal{M}_0^N . Since L_N is a linear operator on the finite-dimensional linear space \mathcal{M}_0^N , the following properties of matrix functions could be utilized on L_N .

Lemma 2.3 ([12]). *Let f be defined on the spectrum of $M \in \mathbb{C}^{d \times d}$, that is, the values*

$$f^{(j)}(\lambda_i), \quad 0 \leq j \leq n_i - 1, \quad 1 \leq i \leq d,$$

exist, where $\{\lambda_i\}_{i=1}^d$ are the eigenvalues of M , and n_i is the order of the largest Jordan block where λ_i appears. Then

- (1) $f(M)$ commutes with M ;
- (2) $f(M^T) = f(M)^T$;
- (3) the eigenvalues of $f(M)$ are $f(\lambda_i)$, $1 \leq i \leq d$;
- (4) $f(P^{-1}MP) = P^{-1}f(M)P$ for any nonsingular matrix $P \in \mathbb{C}^{d \times d}$;
- (5) for any $P, Q \in \mathbb{C}^{d \times d}$, $e^{(P+Q)t} = e^{Pt}e^{Qt} = e^{Qt}e^{Pt}$ if and only if $PQ = QP$;
- (6) $\frac{d}{dt}(e^{Mt}) = Me^{Mt} = e^{Mt}M$.

Remark 2.4. We know that real symmetric matrices are diagonalizable, i.e., each Jordan block is of order 1. Thus, a function f is defined on the spectrum of a symmetric matrix $M \in \mathbb{R}^{d \times d}$ as long as the values $\{f(\lambda_i) : 1 \leq i \leq d\}$ exist.

The space-discrete scheme for the equation (2.3) is to find a function $\tilde{u} : [0, T] \rightarrow \mathcal{M}_0^N$ such that

$$(2.4) \quad \begin{cases} \frac{d\tilde{u}}{dt} = -L_N \tilde{u} - f_N(\tilde{u}), & t \in (0, T], \\ \tilde{u}(0) = u_0, \end{cases}$$

where $u_0 \in \mathcal{M}_0^N$ is given and $f_N(\tilde{u}) = \nabla_N \cdot \left(\frac{\nabla_N \tilde{u}}{1 + |\nabla_N \tilde{u}|^2} \right) + \kappa \Delta_N \tilde{u}$. According to Lemma 2.3, acting as the operator $e^{L_N t}$ on both sides of (2.4) leads to

$$(2.5) \quad \frac{d(e^{L_N t} \tilde{u})}{dt} = -e^{L_N t} f_N(\tilde{u}).$$

Given a positive integer N_t , we divide the time interval by $t_n = n\Delta t$, $0 \leq n \leq N_t$, with a uniform time step $\Delta t = \frac{T}{N_t}$. Then integrating the equation (2.5) from t_n to t_{n+1} gives us

$$(2.6) \quad \tilde{u}(t_{n+1}) = e^{-L_N \Delta t} \tilde{u}(t_n) - \int_0^{\Delta t} e^{-L_N(\Delta t - \tau)} f_N(\tilde{u}(t_n + \tau)) d\tau.$$

The equation (2.6) is equivalent to (2.4) and will play a key role in designing ETD schemes for time stepping.

Remark 2.5. If we approximate the integration using the left-rectangle quadrature and the exponential by $e^{L_{\mathcal{N}}\Delta t} \approx I + L_{\mathcal{N}}\Delta t$ in (2.6), then we obtain

$$(I + L_{\mathcal{N}}\Delta t)\tilde{u}(t_{n+1}) \approx \tilde{u}(t_n) - \Delta t f_{\mathcal{N}}(\tilde{u}(t_n)),$$

which leads to the first order stabilized semi-implicit (SSI1) scheme for solving (2.3)

$$(2.7) \quad \frac{u^{n+1} - u^n}{\Delta t} = -L_{\mathcal{N}}u^{n+1} - f_{\mathcal{N}}(u^n).$$

In particular, the convex splitting scheme proposed in [2] is identical to (2.7) with $\kappa = 1$.

2.3. ETD multistep approximations for time integration. We take an explicit multistep approach to evaluate the time integral on the right-hand side of (2.6). We use the Lagrange polynomial interpolation of degree r based on the nodes $\{t_{n-r}, t_{n-r+1}, \dots, t_n\}$ to approximate $F_{\mathcal{N}}(t_n + \tau) = f_{\mathcal{N}}(\tilde{u}(t_n + \tau))$. Define

$$P_r(\tau) = \sum_{s=0}^r F_{\mathcal{N}}(t_{n-s})\ell_{r,s}(\tau), \quad \tau \in [-r\Delta t, \Delta t],$$

where $\{\ell_{r,s}(\tau)\}_{s=0}^r$ are the standard Lagrange basis functions associated with the nodes $\{t_{n-s}\}_{s=0}^r$. We have the interpolation error $F_{\mathcal{N}}(t_n + \tau) - P_r(\tau) = \mathcal{O}(\Delta t^{r+1})$ if the derivative $F_{\mathcal{N}}^{(r+1)}(t)$ is bounded. The integral in (2.6) can be approximated by

$$\int_0^{\Delta t} e^{-L_{\mathcal{N}}(\Delta t - \tau)} f_{\mathcal{N}}(u(t_n + \tau)) \, d\tau \approx \sum_{s=0}^r S_{r,s}(L_{\mathcal{N}})F_{\mathcal{N}}(t_{n-s}),$$

where

$$S_{r,s}(a) = \int_0^{\Delta t} \ell_{r,s}(\tau)e^{-a(\Delta t - \tau)} \, d\tau, \quad a \in \mathbb{R}.$$

Then we obtain the fully discrete ETD multistep (ETDMs) scheme for solving (2.3) as

$$(2.8) \quad u^{n+1} = e^{-L_{\mathcal{N}}\Delta t}u^n - \sum_{s=0}^r S_{r,s}(L_{\mathcal{N}})f_{\mathcal{N}}(u^{n-s}).$$

This scheme is expected to be $(r + 1)$ -th order accurate in time. We have

$$\tilde{L}_{\mathcal{N}} = \varepsilon^2(D_x^2 + D_y^2)^2 - \kappa(D_x^2 + D_y^2) = P^{-1}(\varepsilon^2(\widehat{D}_x^2 + \widehat{D}_y^2)^2 - \kappa(\widehat{D}_x^2 + \widehat{D}_y^2))P = P^{-1}\widehat{L}_{\mathcal{N}}P,$$

where the operator $\widehat{L}_{\mathcal{N}} = \varepsilon^2(\widehat{D}_x^2 + \widehat{D}_y^2)^2 - \kappa(\widehat{D}_x^2 + \widehat{D}_y^2)$ can be expressed as

$$(\widehat{L}_{\mathcal{N}}\hat{f})_{kl} = \lambda_{kl}\hat{f}_{kl}, \quad (k, l) \in \widehat{J}_{\mathcal{N}},$$

for any $\hat{f} \in \widehat{\mathcal{M}}^{\mathcal{N}}$, where $\{\lambda_{kl} \mid (k, l) \in \widehat{J}_{\mathcal{N}}\}$ are the eigenvalues of $\widehat{L}_{\mathcal{N}}$ (also $\tilde{L}_{\mathcal{N}}$), that is,

$$(2.9) \quad \lambda_{kl} = \varepsilon^2\left(\frac{4k^2\pi^2}{X^2} + \frac{4l^2\pi^2}{Y^2}\right)^2 + \kappa\left(\frac{4k^2\pi^2}{X^2} + \frac{4l^2\pi^2}{Y^2}\right) \geq 0.$$

Noting the definition $L_{\mathcal{N}} = \tilde{L}_{\mathcal{N}}|_{\mathcal{M}_0^{\mathcal{N}}}$ and the fact that all of the eigenvectors belonging to the nonzero eigenvalues of $\tilde{L}_{\mathcal{N}}$ are exactly the eigenvectors of $L_{\mathcal{N}}$, we know that the eigenvalues of $L_{\mathcal{N}}$ are $\{\lambda_{kl} \mid (k, l) \in \widehat{J}_{\mathcal{N}} \setminus (0, 0)\}$. Denoting $\widehat{L}_{\mathcal{N}}^0 = PL_{\mathcal{N}}P^{-1}$,

we finally obtain an implementation formula for the ETD multistep scheme (2.8) as

$$\begin{aligned} u^{n+1} &= P^{-1}e^{-\widehat{L}_N^0\Delta t}Pu^n - \sum_{s=0}^r P^{-1}S_{r,s}(\widehat{L}_N^0)Pf_N(u^{n-s}) \\ &= P^{-1}\left(e^{-\widehat{L}_N^0\Delta t}Pu^n - \sum_{s=0}^r S_{r,s}(\widehat{L}_N^0)Pf_N(u^{n-s})\right), \end{aligned}$$

where

$$(e^{-\widehat{L}_N^0\Delta t}\hat{f})_{kl} = e^{-\lambda_{kl}\Delta t}\hat{f}_{kl}, \quad (S_{r,s}(\widehat{L}_N^0)\hat{f})_{kl} = S_{r,s}(\lambda_{kl})\hat{f}_{kl}, \quad (k, l) \in \widehat{J}_N \setminus (0, 0),$$

for any $\hat{f} \in \widehat{\mathcal{M}}^N$ with $\hat{f}_{00} = 0$. The operators P and P^{-1} can be implemented by the 2-D fast Fourier transform and the corresponding inverse transform, respectively. Therefore, the overall computational complexity is $\mathcal{O}(N^2 \log_2 N)$ per time step, where $N = \max\{N_x, N_y\}$.

We also especially remark that the operator $S_{r,s}(L_N)$ does not depend on time in the case of uniform time partition. Since

$$\ell_{r,s}(\tau) = \prod_{q=0, q \neq s}^r \frac{q\Delta t + \tau}{q\Delta t - s\Delta t} = \prod_{q=0, q \neq s}^r \frac{q + \theta}{q - s} = \sum_{p=0}^r \alpha_p^{r,s} \theta^p,$$

where $\theta = \frac{\tau}{\Delta t}$ and $\{\alpha_p^{r,s}\}_{p=0}^r$ are the coefficients of the polynomial $\ell_{r,s}(\tau)$, we have

$$S_{r,s}(a) = \sum_{p=0}^r \frac{\alpha_p^{r,s}}{(\Delta t)^p} \int_0^{\Delta t} \tau^p e^{-a(\Delta t - \tau)} d\tau = \sum_{p=0}^r \alpha_p^{r,s} \phi_p(a), \quad 0 \leq s \leq r,$$

where

$$\phi_p(a) = \frac{1}{(\Delta t)^p} \int_0^{\Delta t} \tau^p e^{-a(\Delta t - \tau)} d\tau, \quad 0 \leq p \leq r,$$

can be calculated by the recurrence formula

$$\begin{cases} \phi_0(a) = a^{-1}(1 - e^{-a\Delta t}), & \phi_p(a) = a^{-1}\left(1 - \frac{p}{\Delta t}\phi_{p-1}(a)\right), & a \neq 0, \\ \phi_p(a) = \frac{\Delta t}{p+1}, & & a = 0. \end{cases}$$

For the cases $r = 0$ and $r = 1$, we have

$$\ell_{0,0}(\tau) = 1, \quad \ell_{1,0}(\tau) = 1 + \frac{\tau}{\Delta t}, \quad \ell_{1,1}(\tau) = -\frac{\tau}{\Delta t},$$

and the operators $S_{r,s}(L_N)$ can be expressed as follows:

$$S_{0,0}(L_N) = \phi_0(L_N), \quad S_{1,0}(L_N) = \phi_0(L_N) + \phi_1(L_N), \quad S_{1,1}(L_N) = -\phi_1(L_N),$$

where

$$\phi_0(L_N) = L_N^{-1}(I - e^{-L_N\Delta t}), \quad \phi_1(L_N) = L_N^{-1}(I - (L_N\Delta t)^{-1}(I - e^{-L_N\Delta t})).$$

Thus we obtain the first order ETD multistep scheme (ETD1) as

$$\begin{aligned} (2.10) \quad u^{n+1} &= e^{-L_N\Delta t}u^n - \phi_0(L_N)f_N(u^n) \\ &= P^{-1}\left[e^{-\widehat{L}_N^0\Delta t}Pu^n - \phi_0(\widehat{L}_N^0)Pf_N(u^n)\right] \end{aligned}$$

and the second order ETD multistep scheme (ETDMs2) as

$$\begin{aligned}
 (2.11) \quad u^{n+1} &= e^{-L_{\mathcal{N}}\Delta t}u^n - \phi_0(L_{\mathcal{N}})f_{\mathcal{N}}(u^n) - \phi_1(L_{\mathcal{N}})(f_{\mathcal{N}}(u^n) - f_{\mathcal{N}}(u^{n-1})) \\
 &= P^{-1}\left[e^{-\widehat{L}_{\mathcal{N}}^0\Delta t}Pu^n - \phi_0(\widehat{L}_{\mathcal{N}}^0)Pf_{\mathcal{N}}(u^n) - \phi_1(\widehat{L}_{\mathcal{N}}^0)P(f_{\mathcal{N}}(u^n) - f_{\mathcal{N}}(u^{n-1}))\right].
 \end{aligned}$$

Proposition 2.6 (Discrete mass conservation). *The ETD1 scheme (2.10) and the ETDMs2 scheme (2.11) are mass conservative in the discrete sense, i.e., $(u^{n+1} - u^n, 1)_{\mathcal{N}} = 0$ for $0 \leq n \leq N_t - 1$.*

Proof. We just take care of the ETD1 scheme, and the other case is similar. We know from (2.10) that

$$(2.12) \quad u^{n+1} - u^n = -(I - e^{-L_{\mathcal{N}}\Delta t})u^n - L_{\mathcal{N}}^{-1}(I - e^{-L_{\mathcal{N}}\Delta t})f_{\mathcal{N}}(u^n).$$

Define $g_1(a) = 1 - e^{-a\Delta t}$ for $a \in \mathbb{R}$ and an operator $B_1 = g_1(L_{\mathcal{N}}) = I - e^{-L_{\mathcal{N}}\Delta t}$. Since $L_{\mathcal{N}}$ is symmetric positive definite and $0 < g_1(a) < 1$ for any $a > 0$, we know from Lemma 2.3 that B_1 is also symmetric positive definite and commutes with $L_{\mathcal{N}}$ and $L_{\mathcal{N}}^{-1}$. Then we obtain from (2.12) that

$$u^{n+1} - u^n = -B_1u^n - L_{\mathcal{N}}^{-1}B_1f_{\mathcal{N}}(u^n) = -B_1(u^n + L_{\mathcal{N}}^{-1}f_{\mathcal{N}}(u^n)).$$

Taking the discrete L^2 inner product of the above with the constant $v \equiv 1$ and using the symmetry of B_1 , we obtain

$$(u^{n+1} - u^n, 1)_{\mathcal{N}} = -(u^n + L_{\mathcal{N}}^{-1}f_{\mathcal{N}}(u^n), B_1v)_{\mathcal{N}}.$$

Note that

$$B_1 = I - e^{-L_{\mathcal{N}}\Delta t} = L_{\mathcal{N}}\Delta t - \frac{1}{2}(L_{\mathcal{N}}\Delta t)^2 + \frac{1}{6}(L_{\mathcal{N}}\Delta t)^3 + \dots;$$

therefore B_1 is essentially a differential operator, and thus $B_1v \equiv 0$, which completes the proof. □

3. ENERGY STABILITY

For a linear symmetric positive definite operator $\mathcal{A} : \mathcal{M}^{\mathcal{N}} \rightarrow \mathcal{M}^{\mathcal{N}}$, we denote by $\sigma(\mathcal{A})$ the set of all the eigenvalues of \mathcal{A} , and define the norm of \mathcal{A} as the spectrum radius of \mathcal{A} , that is, $\|\mathcal{A}\| = \max\{|\lambda| : \lambda \in \sigma(\mathcal{A})\}$. It obviously holds that

$$\|\mathcal{A}v\|_{\mathcal{N}} \leq \|\mathcal{A}\|\|v\|_{\mathcal{N}} \quad \forall v \in \mathcal{M}^{\mathcal{N}}.$$

The discrete energy functional corresponding to the continuous one $E(u)$ can be defined as

$$(3.1) \quad E_{\mathcal{N}}(u) = \left(-\frac{1}{2} \ln(1 + |\nabla_{\mathcal{N}}u|^2), 1\right)_{\mathcal{N}} + \frac{\varepsilon^2}{2} \|\Delta_{\mathcal{N}}u\|_{\mathcal{N}}^2$$

for any $u \in \mathcal{M}^{\mathcal{N}}$.

Lemma 3.1. *For any $v, w \in \mathcal{M}_0^{\mathcal{N}}$, it holds that*

$$E_{\mathcal{N}}(v) - E_{\mathcal{N}}(w) \leq (L_{\mathcal{N}}v + f_{\mathcal{N}}(w), v - w)_{\mathcal{N}}.$$

Proof. According to Proposition 2.1, a convex splitting of the discrete energy (3.1) can be given by $E_{\mathcal{N}}(u) = E_{\mathcal{N},c}(u) - E_{\mathcal{N},e}(u)$ with

$$E_{\mathcal{N},c}(u) = \frac{\kappa}{2} \|\nabla_{\mathcal{N}} u\|_{\mathcal{N}}^2 + \frac{\varepsilon^2}{2} \|\Delta_{\mathcal{N}} u\|_{\mathcal{N}}^2,$$

$$E_{\mathcal{N},e}(u) = \frac{\kappa}{2} \|\nabla_{\mathcal{N}} u\|_{\mathcal{N}}^2 + \left(\frac{1}{2} \ln(1 + |\nabla_{\mathcal{N}} u|^2), 1 \right)_{\mathcal{N}},$$

which are the corresponding discrete versions of E_c and E_e , respectively. Using the convexity of $E_{\mathcal{N},c}$ and $E_{\mathcal{N},e}$, we have the following inequality (see [20, Lemma 3.9] or [31, Theorem 3.5]):

$$E_{\mathcal{N}}(v) - E_{\mathcal{N}}(w) \leq (\delta_u E_{\mathcal{N},c}(v) - \delta_u E_{\mathcal{N},e}(w), v - w)_{\mathcal{N}}.$$

Some careful calculations give the variational derivatives

$$\delta_u E_{\mathcal{N},c}(v) = L_{\mathcal{N}} v, \quad \delta_u E_{\mathcal{N},e}(w) = -f_{\mathcal{N}}(w),$$

which completes the proof. □

Theorem 3.2. *The approximate solution produced by the ETD1 scheme (2.10) satisfies the energy inequality*

$$(3.2) \quad E_{\mathcal{N}}(u^{n+1}) \leq E_{\mathcal{N}}(u^n)$$

for any time step size $\Delta t > 0$, i.e., the ETD1 scheme (2.10) is unconditionally energy stable.

Proof. Recall the ETD1 scheme (2.10), that is,

$$u^{n+1} = e^{-L_{\mathcal{N}} \Delta t} u^n - L_{\mathcal{N}}^{-1} B_1 f_{\mathcal{N}}(u^n).$$

Thus we have

$$\begin{aligned} f_{\mathcal{N}}(u^n) &= -B_1^{-1} L_{\mathcal{N}}(u^{n+1} - e^{-L_{\mathcal{N}} \Delta t} u^n) \\ &= -B_1^{-1} L_{\mathcal{N}}(u^{n+1} - u^n + (I - e^{-L_{\mathcal{N}} \Delta t}) u^n) \\ &= -B_1^{-1} L_{\mathcal{N}}(u^{n+1} - u^n) - B_1^{-1} L_{\mathcal{N}} B_1 u^n \\ &= -B_1^{-1} L_{\mathcal{N}}(u^{n+1} - u^n) - L_{\mathcal{N}} u^n. \end{aligned}$$

Define $g_2(a) = \left(\frac{1}{g_1(a)} - 1\right)a$ for $a \neq 0$ and an operator $B_2 = g_2(L_{\mathcal{N}}) = (B_1^{-1} - I)L_{\mathcal{N}}$. For any $a > 0$, we have $0 < g_1(a) < 1$ and thus $g_2(a) > 0$. Therefore, $(B_1^{-1} - I)L_{\mathcal{N}}$ is symmetric positive definite. Setting $v = u^{n+1}$ and $w = u^n$ in Lemma 3.1, we obtain

$$(3.3) \quad \begin{aligned} E_{\mathcal{N}}(u^{n+1}) - E_{\mathcal{N}}(u^n) &\leq (L_{\mathcal{N}} u^{n+1} + f_{\mathcal{N}}(u^n), u^{n+1} - u^n)_{\mathcal{N}} \\ &= (-B_1^{-1} L_{\mathcal{N}}(u^{n+1} - u^n) + L_{\mathcal{N}}(u^{n+1} - u^n), u^{n+1} - u^n)_{\mathcal{N}} \\ &= -(B_2(u^{n+1} - u^n), u^{n+1} - u^n)_{\mathcal{N}}. \end{aligned}$$

Proposition 2.6 tells us that $u^{n+1} - u^n \in \mathcal{M}_0^{\mathcal{N}}$, so the energy inequality (3.2) comes from (3.3) and the fact that B_2 is positive definite. □

Corollary 3.3. *For the numerical solution $\{u^n\}_{n=1}^{N_t}$ produced by the ETD1 scheme (2.10) with the starting data u^0 , there exists a constant C depending only on ε and $|\Omega|$ such that*

$$\max_{1 \leq n \leq N_t} \|\Delta_{\mathcal{N}} u^n\|_{\mathcal{N}} \leq \frac{2}{\varepsilon} \sqrt{E_{\mathcal{N}}(u^0) + C}.$$

Proof. For any $y \geq 0$ and $\alpha \geq 0$, it holds that

$$\ln(1 + y) + \ln \alpha = \ln(1 + (\alpha y + \alpha - 1)) \leq \alpha y + \alpha - 1,$$

namely,

$$\ln(1 + y) \leq \alpha y - \ln \alpha + \alpha - 1;$$

then we obtain

$$E_{\mathcal{N}}(u^n) \geq -\frac{\alpha}{2} \|\nabla_{\mathcal{N}} u^n\|_{\mathcal{N}}^2 - \frac{1}{2}(-\ln \alpha + \alpha - 1, 1)_{\mathcal{N}} + \frac{\varepsilon^2}{2} \|\Delta_{\mathcal{N}} u^n\|_{\mathcal{N}}^2.$$

Since $u^n \in \mathcal{M}_0^{\mathcal{N}}$, we have the following discrete Poincaré inequality:

$$\|\nabla_{\mathcal{N}} u^n\|_{\mathcal{N}}^2 \leq \frac{XY}{4\pi^2} \|\Delta_{\mathcal{N}} u^n\|_{\mathcal{N}}^2.$$

Choosing $\alpha = \frac{2\pi^2\varepsilon^2}{XY}$ and denoting $C_\alpha = \frac{1}{2}(-\ln \alpha + \alpha - 1)$, we derive

$$E_{\mathcal{N}}(u^n) \geq \frac{\varepsilon^2}{4} \|\Delta_{\mathcal{N}} u^n\|_{\mathcal{N}}^2 - C_\alpha XY.$$

Using Theorem 3.2, we have $E_{\mathcal{N}}(u^n) \leq E_{\mathcal{N}}(u^{n-1}) \leq \dots \leq E_{\mathcal{N}}(u^0)$; then

$$\frac{\varepsilon^2}{4} \|\Delta_{\mathcal{N}} u^n\|_{\mathcal{N}}^2 \leq E_{\mathcal{N}}(u^0) + C_\alpha XY,$$

which completes the proof. □

Remark 3.4. We know from Corollary 3.3 that the numerical solution to the ETD1 scheme (2.10) is uniformly bounded in time in the discrete H^2 sense. Such uniform bounds were also achieved for the nonlinear and linear convex splitting schemes given in [2, 30]. By comparison, in some other related works (see, e.g., [22]), the energy stability is considered with respect to energy involved artificial variables. As a result, although the energy stability is obtained at the numerical level, a uniform in time H^2 bound of the numerical solution could hardly be justified at the theoretical level. Therefore, Corollary 3.3 implies one of the key advantages of the ETD1 scheme (2.10).

Now we turn to the energy stability of the ETDMs2 scheme. Define a mapping $\beta : \mathbb{R}^2 \rightarrow \mathbb{R}^2$ as

$$(3.4) \quad \beta(\mathbf{v}) = \frac{\mathbf{v}}{1 + |\mathbf{v}|^2}.$$

Lemma 3.5. *For any $\mathbf{v}, \mathbf{w} \in \mathbb{R}^2$, there exists a symmetric matrix $Q \in \mathbb{R}^{2 \times 2}$ such that*

$$\beta(\mathbf{v}) - \beta(\mathbf{w}) = Q(\mathbf{v} - \mathbf{w}),$$

and the eigenvalues λ_1, λ_2 of Q satisfy $-\frac{1}{8} \leq \lambda_1, \lambda_2 \leq 1$. Consequently, it holds that

$$(3.5) \quad |\beta(\mathbf{v}) - \beta(\mathbf{w})| \leq |\mathbf{v} - \mathbf{w}| \quad \forall \mathbf{v}, \mathbf{w} \in \mathbb{R}^2.$$

Proof. The Jacobian matrix of β at $\mathbf{v} = (v_1, v_2)$ is

$$\nabla \beta(\mathbf{v}) = \frac{1}{(1 + |\mathbf{v}|^2)^2} \begin{pmatrix} 1 - v_1^2 + v_2^2 & -2v_1v_2 \\ -2v_1v_2 & 1 + v_1^2 - v_2^2 \end{pmatrix}$$

and the eigenvalues of $\nabla \beta(\mathbf{v})$ are

$$\mu_1(\mathbf{v}) = \frac{1 - |\mathbf{v}|^2}{(1 + |\mathbf{v}|^2)^2}, \quad \mu_2(\mathbf{v}) = \frac{1}{1 + |\mathbf{v}|^2}.$$

Since $\min_{\alpha \geq 0} \frac{1-\alpha}{(1+\alpha)^2} = -\frac{1}{8}$, we have

$$(3.6) \quad -\frac{1}{8} \leq \mu_1(\mathbf{v}) \leq \mu_2(\mathbf{v}) \leq 1.$$

For any $\mathbf{v}, \mathbf{w} \in \mathbb{R}^2$, the Taylor formula gives us

$$\beta(\mathbf{v}) - \beta(\mathbf{w}) = Q(\mathbf{v} - \mathbf{w}), \quad Q = \int_0^1 \nabla\beta(\theta\mathbf{v} + (1-\theta)\mathbf{w}) \, d\theta.$$

The symmetry of $\nabla\beta$ implies the symmetry of Q , so there exists an orthonormal matrix $P_\theta = \begin{pmatrix} a_\theta & b_\theta \\ c_\theta & d_\theta \end{pmatrix}$ such that

$$\begin{pmatrix} \lambda_1 & \\ & \lambda_2 \end{pmatrix} = \int_0^1 \begin{pmatrix} a_\theta & b_\theta \\ c_\theta & d_\theta \end{pmatrix} \begin{pmatrix} \mu_1(\boldsymbol{\xi}_\theta) & \\ & \mu_2(\boldsymbol{\xi}_\theta) \end{pmatrix} \begin{pmatrix} a_\theta & c_\theta \\ b_\theta & d_\theta \end{pmatrix} \, d\theta,$$

where $\boldsymbol{\xi}_\theta = \theta\mathbf{v} + (1-\theta)\mathbf{w}$, λ_1 and λ_2 are the eigenvalues of Q , which leads to

$$\lambda_1 = \int_0^1 (a_\theta^2 \mu_1(\boldsymbol{\xi}_\theta) + b_\theta^2 \mu_2(\boldsymbol{\xi}_\theta)) \, d\theta, \quad \lambda_2 = \int_0^1 (c_\theta^2 \mu_1(\boldsymbol{\xi}_\theta) + d_\theta^2 \mu_2(\boldsymbol{\xi}_\theta)) \, d\theta.$$

The fact $a_\theta^2 + b_\theta^2 = c_\theta^2 + d_\theta^2 = 1$ implies that

$$\mu_1(\boldsymbol{\xi}_\theta) \leq \lambda_1 \leq \mu_2(\boldsymbol{\xi}_\theta), \quad \mu_1(\boldsymbol{\xi}_\theta) \leq \lambda_2 \leq \mu_2(\boldsymbol{\xi}_\theta),$$

which gives us $-\frac{1}{8} \leq \lambda_1, \lambda_2 \leq 1$ by combining with (3.6). In addition, since the 2-norm of a symmetric matrix is equal to its spectrum radius, we obtain (3.5). \square

Theorem 3.6. *The approximate solution produced by the ETDMs2 scheme (2.11) satisfies*

$$(3.7) \quad E_{\mathcal{N}}(u^{n+1}) \leq E_{\mathcal{N}}(u^n) + \frac{1+\kappa}{2} (\|\nabla_{\mathcal{N}}(u^{n+1} - u^n)\|_{\mathcal{N}}^2 + \|\nabla_{\mathcal{N}}(u^n - u^{n-1})\|_{\mathcal{N}}^2)$$

for any time step size $\Delta t > 0$.

Proof. Recall the ETDMs2 scheme (2.11), that is,

$$u^{n+1} = e^{-L_{\mathcal{N}}\Delta t} u^n - L_{\mathcal{N}}^{-1} B_1 f_{\mathcal{N}}(u^n) - L_{\mathcal{N}}^{-1} (I - (L_{\mathcal{N}}\Delta t)^{-1} B_1) (f_{\mathcal{N}}(u^n) - f_{\mathcal{N}}(u^{n-1})).$$

Then we have

$$\begin{aligned} f_{\mathcal{N}}(u^n) &= -B_1^{-1} L_{\mathcal{N}} (u^{n+1} - e^{-L_{\mathcal{N}}\Delta t} u^n) \\ &\quad - B_1^{-1} (I - (L_{\mathcal{N}}\Delta t)^{-1} B_1) (f_{\mathcal{N}}(u^n) - f_{\mathcal{N}}(u^{n-1})) \\ &= -B_1^{-1} L_{\mathcal{N}} (u^{n+1} - u^n) \\ &\quad - B_1^{-1} L_{\mathcal{N}} B_1 u^n - B_1^{-1} (I - (L_{\mathcal{N}}\Delta t)^{-1} B_1) (f_{\mathcal{N}}(u^n) - f_{\mathcal{N}}(u^{n-1})) \\ &= -B_1^{-1} L_{\mathcal{N}} (u^{n+1} - u^n) - L_{\mathcal{N}} u^n \\ &\quad - (B_1^{-1} - (L_{\mathcal{N}}\Delta t)^{-1}) (f_{\mathcal{N}}(u^n) - f_{\mathcal{N}}(u^{n-1})). \end{aligned}$$

Define $g_3(a) = (1 - e^{-a\Delta t})^{-1} - (a\Delta t)^{-1}$ for $a \neq 0$ and an operator $B_3 = g_3(L_{\mathcal{N}}) = B_1^{-1} - (L_{\mathcal{N}}\Delta t)^{-1}$. It is easy to show that $g_3(a) = 1 + (e^{a\Delta t} - 1)^{-1} - (a\Delta t)^{-1}$ and thus $0 < g_3(a) \leq 1$ for any $a > 0$, which implies that B_3 is symmetric positive definite and $\|B_3\| \leq 1$. Using Lemma 3.1, we get

$$E_{\mathcal{N}}(u^{n+1}) - E_{\mathcal{N}}(u^n) \leq (L_{\mathcal{N}} u^{n+1} + f_{\mathcal{N}}(u^n), u^{n+1} - u^n)_{\mathcal{N}} = S_1 + S_2,$$

where

$$\begin{aligned} S_1 &= -((B_2(u^{n+1} - u^n), u^{n+1} - u^n)_{\mathcal{N}}), \\ S_2 &= -(B_3(f_{\mathcal{N}}(u^n) - f_{\mathcal{N}}(u^{n-1})), u^{n+1} - u^n)_{\mathcal{N}}. \end{aligned}$$

First it is obvious that $S_1 \leq 0$ since B_2 is positive definite. Note that B_3 is symmetric and commutes with $\nabla_{\mathcal{N}}$, thus we have

$$\begin{aligned} S_2 &= -(f_{\mathcal{N}}(u^n) - f_{\mathcal{N}}(u^{n-1}), B_3(u^{n+1} - u^n))_{\mathcal{N}} \\ &= -(\nabla_{\mathcal{N}} \cdot (\beta(\nabla_{\mathcal{N}}u^n) - \beta(\nabla_{\mathcal{N}}u^{n-1})) + \kappa\Delta_{\mathcal{N}}(u^n - u^{n-1}), B_3(u^{n+1} - u^n))_{\mathcal{N}} \\ &= (\beta(\nabla_{\mathcal{N}}u^n) - \beta(\nabla_{\mathcal{N}}u^{n-1}) + \kappa\nabla_{\mathcal{N}}(u^n - u^{n-1}), B_3\nabla_{\mathcal{N}}(u^{n+1} - u^n))_{\mathcal{N}} \\ &\leq (\|\beta(\nabla_{\mathcal{N}}u^n) - \beta(\nabla_{\mathcal{N}}u^{n-1})\|_{\mathcal{N}} + \kappa\|\nabla_{\mathcal{N}}(u^n - u^{n-1})\|_{\mathcal{N}})\|B_3\nabla_{\mathcal{N}}(u^{n+1} - u^n)\|_{\mathcal{N}}, \end{aligned}$$

where $\beta : \mathcal{M}^{\mathcal{N}} \times \mathcal{M}^{\mathcal{N}} \rightarrow \mathcal{M}^{\mathcal{N}} \times \mathcal{M}^{\mathcal{N}}$ is defined as (3.4). Denote by $\nabla\beta$ the Fréchet-derivative of β . The Taylor formula gives

$$\beta(\nabla_{\mathcal{N}}u^n) - \beta(\nabla_{\mathcal{N}}u^{n-1}) = Q_n\nabla_{\mathcal{N}}(u^n - u^{n-1}),$$

where

$$Q_n = \int_0^1 \nabla\beta(\theta\nabla_{\mathcal{N}}u^n + (1 - \theta)\nabla_{\mathcal{N}}u^{n-1}) d\theta.$$

We know from Lemma 3.5 that $\|Q_n\| \leq 1$, then

$$\|\beta(\nabla_{\mathcal{N}}u^n) - \beta(\nabla_{\mathcal{N}}u^{n-1})\|_{\mathcal{N}} \leq \|Q_n\| \|\nabla_{\mathcal{N}}(u^n - u^{n-1})\|_{\mathcal{N}} \leq \|\nabla_{\mathcal{N}}(u^n - u^{n-1})\|_{\mathcal{N}}.$$

Using the consistency it also holds that

$$\|B_3\nabla_{\mathcal{N}}(u^{n+1} - u^n)\|_{\mathcal{N}} \leq \|B_3\| \|\nabla_{\mathcal{N}}(u^{n+1} - u^n)\|_{\mathcal{N}} \leq \|\nabla_{\mathcal{N}}(u^{n+1} - u^n)\|_{\mathcal{N}};$$

thus we obtain

$$\begin{aligned} S_2 &\leq (1 + \kappa)\|\nabla_{\mathcal{N}}(u^n - u^{n-1})\|_{\mathcal{N}}\|\nabla_{\mathcal{N}}(u^{n+1} - u^n)\|_{\mathcal{N}} \\ &\leq \frac{1 + \kappa}{2} (\|\nabla_{\mathcal{N}}(u^n - u^{n-1})\|_{\mathcal{N}}^2 + \|\nabla_{\mathcal{N}}(u^{n+1} - u^n)\|_{\mathcal{N}}^2), \end{aligned}$$

which completes the proof of (3.7). □

Remark 3.7. Unlike the first order scheme (2.10), one may fail to derive a uniform H^2 bound for the numerical solution to the second order scheme (2.11), because there are two additional positive terms involved in the energy inequality (3.7) and a direct control of these accumulative correction terms is not available. Similarly, the second order nonlinear and linear schemes developed in [22] also fail to ensure the H^2 stability of the numerical solution. In comparison, for the second order nonlinear convex splitting scheme presented in [27], the uniform H^2 bound of the numerical solution is obtained from the energy stability by assuming that the concave part is a quadratic term.

4. ERROR ESTIMATES

We denote by u_e the exact solution to (1.1). Define

$$H_{\text{per}}^m(\Omega) = \{v \in H^m(\Omega) \mid v \text{ is } \Omega\text{-periodic}\}.$$

Li and Liu [17] have proved that if the initial data $u_e(\cdot, 0) \in H_{\text{per}}^m(\Omega)$ for some integer $m \geq 2$, the solution u_e satisfies

$$u_e \in L^\infty(0, T; H_{\text{per}}^m(\Omega)) \cap L^2(0, T; H_{\text{per}}^{m+2}(\Omega)) \quad \text{and} \quad \partial_t u_e \in L^2(0, T; H_{\text{per}}^{m-2}(\Omega)).$$

We will derive rigorously the error estimates for the ETD1 and ETDMS2 schemes under some assumptions on the regularity of u_e . Denote by $u(t)$ the limitation of $u_e(\cdot, t)$ on the mesh Ω_N at any fixed time t . Let $N = \max\{N_x, N_y\}$. Denoting by λ_{\min} the smallest eigenvalue of L_N , we know from (2.9) that $\lambda_{\min} > 0$.

First, we estimate the error between the exact solution $u(t)$ and the solution $\tilde{u}(t)$ of the space-discrete problem (2.4), i.e.,

$$(4.1) \quad \begin{cases} \frac{d\tilde{u}}{dt} = -\varepsilon^2 \Delta_N^2 \tilde{u} - \nabla_N \cdot \beta(\nabla_N \tilde{u}), & t \in (0, T], \\ \tilde{u}(0) = u(0) \in \mathcal{M}_0^N. \end{cases}$$

Lemma 4.1. *Assume that $u_e \in H^1(0, T; H_{\text{per}}^{m+6}(\Omega))$. For any fixed $t \in (0, T]$, we have*

$$(4.2) \quad \|u(t) - \tilde{u}(t)\|_N \leq C_0 N^{-m},$$

where $C_0 > 0$ is a constant independent on N .

Proof. The exact solution limited on the mesh Ω_N , $u(t)$, could be regarded as satisfying (4.1) with a defect $\delta(t)$

$$(4.3) \quad \frac{du}{dt} = -\varepsilon^2 \Delta_N^2 u - \nabla_N \cdot \beta(\nabla_N u) + \delta(t), \quad t \in (0, T],$$

where $\delta(t) = \varepsilon^2(\Delta_N^2 u - \Delta^2 u_e) + \nabla_N \cdot \beta(\nabla_N u) - \nabla \cdot \beta(\nabla u_e)$. We know from the Sobolev embedding theorem and $u_e \in H^1(0, T; H_{\text{per}}^{m+6}(\Omega))$ that

$$\sup_{t \in (0, T]} \|\delta(t)\|_N \leq C_* N^{-m}.$$

Let $v(t) = u(t) - \tilde{u}(t)$, $t \in [0, T]$, then the difference between (4.3) and (4.1) gives us

$$(4.4) \quad \frac{dv}{dt} = -\varepsilon^2 \Delta_N^2 v - \nabla_N \cdot (\beta(\nabla_N u) - \beta(\nabla_N \tilde{u})) + \delta(t), \quad t \in (0, T],$$

with $v(0) = 0$. According to Lemma 3.5, we have

$$\|\beta(\nabla_N u) - \beta(\nabla_N \tilde{u})\|_N \leq \|\nabla_N u - \nabla_N \tilde{u}\|_N = \|\nabla_N v\|_N.$$

Taking the discrete L^2 inner product of (4.4) with $2v$ and using Proposition 2.2 yield

$$\begin{aligned} \frac{d}{dt} \|v\|_N^2 &= -2\varepsilon^2 \|\Delta_N v\|_N^2 + 2(\beta(\nabla_N u) - \beta(\nabla_N \tilde{u}), \nabla_N v)_N + 2(\delta, v)_N \\ &\leq -2\varepsilon^2 \|\Delta_N v\|_N^2 + 2\|\beta(\nabla_N u) - \beta(\nabla_N \tilde{u})\|_N \|\nabla_N v\|_N + 2(\delta, v)_N \\ &\leq -2\varepsilon^2 \|\Delta_N v\|_N^2 + 2\|\nabla_N v\|_N^2 + 2(\delta, v)_N \\ &\leq -2\varepsilon^2 \|\Delta_N v\|_N^2 + 2\|v\|_N \|\Delta_N v\|_N + 2\|\delta\|_N \|v\|_N \\ &\leq -2\varepsilon^2 \|\Delta_N v\|_N^2 + \frac{1}{2\varepsilon^2} \|v\|_N^2 + 2\varepsilon^2 \|\Delta_N v\|_N^2 + 2\varepsilon^2 \|\delta\|_N^2 + \frac{1}{2\varepsilon^2} \|v\|_N^2 \\ &= \frac{1}{\varepsilon^2} \|v\|_N^2 + 2\varepsilon^2 \|\delta\|_N^2. \end{aligned}$$

An application of the Gronwall inequality then leads to

$$\|v(t)\|_N^2 \leq 2\varepsilon^2 \int_0^t e^{(t-\tau)/\varepsilon^2} \|\delta(\tau)\|_N^2 d\tau \leq 2T\varepsilon^2 e^{T/\varepsilon^2} C_*^2 N^{-2m}, \quad t \in (0, T],$$

which gives (4.2) with $C_0 = C_* \sqrt{2T} \varepsilon e^{T/2\varepsilon^2}$. □

Next, we estimate the error between the space-discrete solution $\tilde{u}(t)$ given by (2.6) (equivalent to (2.4)) and the approximate solution u^n computed by the ETD1 scheme (2.10). Recall $F_{\mathcal{N}}(t) = f_{\mathcal{N}}(\tilde{u}(t))$.

Lemma 4.2. *Assume that $\{u^n\}_{n=1}^{N_t}$ is the approximate solutions calculated by the ETD1 scheme (2.10) with $u^0 = \tilde{u}(0)$. If $(I + L_{\mathcal{N}}\Delta t)F'_{\mathcal{N}} \in L^2(0, T; \mathcal{M}^{\mathcal{N}})$ and the time step size $\Delta t \leq \frac{\varepsilon^2}{4}$, then we have*

$$(4.5) \quad \|\tilde{u}(t_n) - u^n\|_{\mathcal{N}} \leq C_1 \Delta t, \quad 1 \leq n \leq N_t,$$

where $C_1 > 0$ is a constant independent on Δt and N .

Proof. The space-discrete solution $\tilde{u}(t_{n+1})$ could be regarded as satisfying (2.10) with a defect $\delta_{n+1}^{(1)}$,

$$(4.6) \quad \tilde{u}(t_{n+1}) = e^{-L_{\mathcal{N}}\Delta t}\tilde{u}(t_n) - \phi_0(L_{\mathcal{N}})F_{\mathcal{N}}(t_n) - \delta_{n+1}^{(1)}, \quad 0 \leq n \leq N_t - 1,$$

where

$$\begin{aligned} \delta_{n+1}^{(1)} &= \int_0^{\Delta t} e^{-L_{\mathcal{N}}(\Delta t - \tau)}(F_{\mathcal{N}}(t_n + \tau) - F_{\mathcal{N}}(t_n)) \, d\tau \\ &= \int_0^{\Delta t} e^{-L_{\mathcal{N}}(\Delta t - \tau)} \int_0^{\tau} F'_{\mathcal{N}}(t_n + \sigma) \, d\sigma \, d\tau. \end{aligned}$$

Since

$$\begin{aligned} \int_0^{\tau} \|(I + L_{\mathcal{N}}\Delta t)F'_{\mathcal{N}}(t_n + \sigma)\|_{\mathcal{N}} \, d\sigma &= \frac{\tau}{T} \int_0^T \|(I + L_{\mathcal{N}}\Delta t)F'_{\mathcal{N}}(t_n + \frac{\tau}{T}\sigma)\|_{\mathcal{N}} \, d\sigma \\ &\leq \frac{\tau}{T} \left(\int_0^T \|(I + L_{\mathcal{N}}\Delta t)F'_{\mathcal{N}}(t_n + \frac{\tau}{T}\sigma)\|_{\mathcal{N}}^2 \, d\sigma \right)^{\frac{1}{2}} \sqrt{T} \leq \frac{\tau}{\sqrt{T}} M_1, \end{aligned}$$

where $M_1 = \|(I + L_{\mathcal{N}}\Delta t)F'_{\mathcal{N}}\|_{L^2(0, T; \mathcal{M}^{\mathcal{N}})}$, we have

$$\begin{aligned} \|(I + L_{\mathcal{N}}\Delta t)\delta_{n+1}^{(1)}\|_{\mathcal{N}} &\leq \int_0^{\Delta t} \|e^{-L_{\mathcal{N}}(\Delta t - \tau)}\| \int_0^{\tau} \|(I + L_{\mathcal{N}}\Delta t)F'_{\mathcal{N}}(t_n + \sigma)\|_{\mathcal{N}} \, d\sigma \, d\tau \\ &\leq \frac{M_1}{\sqrt{T}} \int_0^{\Delta t} \tau e^{-\lambda_{\min}(\Delta t - \tau)} \, d\tau \\ &= \frac{M_1}{\sqrt{T}} \Delta t^2 \cdot \frac{e^{-\lambda_{\min}\Delta t} - 1 + \lambda_{\min}\Delta t}{(\lambda_{\min}\Delta t)^2} \leq \frac{M_1}{2\sqrt{T}} \Delta t^2. \end{aligned}$$

Let $v^n = \tilde{u}(t_n) - u^n$, $1 \leq n \leq N_t$. The difference between (2.10) and (4.6) gives

$$(4.7) \quad v^{n+1} = e^{-L_{\mathcal{N}}\Delta t}v^n - \phi_0(L_{\mathcal{N}})(f_{\mathcal{N}}(\tilde{u}(t_n)) - f_{\mathcal{N}}(u^n)) - \delta_{n+1}^{(1)}, \quad 0 \leq n \leq N_t - 1,$$

with $v^0 = 0$. Acting $(I + L_{\mathcal{N}}\Delta t)$ on both sides of (4.7) and taking the discrete L^2 inner product with v^{n+1} yield

$$(4.8) \quad \|v^{n+1}\|_{\mathcal{N}}^2 + \varepsilon^2 \Delta t \|\Delta_{\mathcal{N}}v^{n+1}\|_{\mathcal{N}}^2 + \kappa \Delta t \|\nabla_{\mathcal{N}}v^{n+1}\|_{\mathcal{N}}^2 = \text{RHS}, \quad 0 \leq n \leq N_t - 1,$$

where

$$\text{RHS} = (q_1(L_{\mathcal{N}}\Delta t)v^n - q_2(L_{\mathcal{N}}\Delta t)\Delta t(f_{\mathcal{N}}(\tilde{u}(t_n)) - f_{\mathcal{N}}(u^n)) - (I + L_{\mathcal{N}}\Delta t)\delta_{n+1}^{(1)}, v^{n+1})_{\mathcal{N}}$$

with

$$q_1(a) = (1 + a)e^{-a}, \quad q_2(a) = \frac{(1 + a)(1 - e^{-a})}{a}.$$

It is easy to show that $0 < q_1(a) < 1 < q_2(a) < 2$ for any $a > 0$, thus

$$\begin{aligned}
 \text{RHS} &= (q_1(L_{\mathcal{N}}\Delta t)v^n, v^{n+1})_{\mathcal{N}} \\
 &\quad + \Delta t(q_2(L_{\mathcal{N}}\Delta t)(\beta(\nabla_{\mathcal{N}}\tilde{u}(t_n)) - \beta(\nabla_{\mathcal{N}}u^n)), \nabla_{\mathcal{N}}v^{n+1})_{\mathcal{N}} \\
 &\quad + \kappa\Delta t(q_2(L_{\mathcal{N}}\Delta t)\nabla_{\mathcal{N}}v^n, \nabla_{\mathcal{N}}v^{n+1})_{\mathcal{N}} - ((I + L_{\mathcal{N}}\Delta t)\delta_{n+1}^{(1)}, v^{n+1})_{\mathcal{N}} \\
 &\leq \|q_1(L_{\mathcal{N}}\Delta t)\| \|v^n\|_{\mathcal{N}} \|v^{n+1}\|_{\mathcal{N}} + (1+\kappa)\Delta t \|q_2(L_{\mathcal{N}}\Delta t)\| \|\nabla_{\mathcal{N}}v^n\|_{\mathcal{N}} \|\nabla_{\mathcal{N}}v^{n+1}\|_{\mathcal{N}} \\
 &\quad + \|(I + L_{\mathcal{N}}\Delta t)\delta_{n+1}^{(1)}\|_{\mathcal{N}} \|v^{n+1}\|_{\mathcal{N}} \\
 &\leq \|v^n\|_{\mathcal{N}} \|v^{n+1}\|_{\mathcal{N}} + 2(1+\kappa)\Delta t \|\nabla_{\mathcal{N}}v^n\|_{\mathcal{N}} \|\nabla_{\mathcal{N}}v^{n+1}\|_{\mathcal{N}} \\
 &\quad + \|(I + L_{\mathcal{N}}\Delta t)\delta_{n+1}^{(1)}\|_{\mathcal{N}} \|v^{n+1}\|_{\mathcal{N}} \\
 &\leq \frac{1}{2}\|v^n\|_{\mathcal{N}}^2 + \frac{1}{2}\|v^{n+1}\|_{\mathcal{N}}^2 + (1+\kappa)\Delta t \|\nabla_{\mathcal{N}}v^n\|_{\mathcal{N}}^2 + (1+\kappa)\Delta t \|\nabla_{\mathcal{N}}v^{n+1}\|_{\mathcal{N}}^2 \\
 &\quad + \|(I + L_{\mathcal{N}}\Delta t)\delta_{n+1}^{(1)}\|_{\mathcal{N}} \|v^{n+1}\|_{\mathcal{N}}.
 \end{aligned}$$

Then we get by combining the above equation with (4.8) that

$$\begin{aligned}
 &\frac{1}{2}(\|v^{n+1}\|_{\mathcal{N}}^2 - \|v^n\|_{\mathcal{N}}^2) + \varepsilon^2\Delta t \|\Delta_{\mathcal{N}}v^{n+1}\|_{\mathcal{N}}^2 \\
 &\leq (1+\kappa)\Delta t \|\nabla_{\mathcal{N}}v^n\|_{\mathcal{N}}^2 + \Delta t \|\nabla_{\mathcal{N}}v^{n+1}\|_{\mathcal{N}}^2 + \|(I + L_{\mathcal{N}}\Delta t)\delta_{n+1}^{(1)}\|_{\mathcal{N}} \|v^{n+1}\|_{\mathcal{N}} \\
 &\leq (1+\kappa)\Delta t \|v^n\|_{\mathcal{N}} \|\Delta_{\mathcal{N}}v^n\|_{\mathcal{N}} + \Delta t \|v^{n+1}\|_{\mathcal{N}} \|\Delta_{\mathcal{N}}v^{n+1}\|_{\mathcal{N}} \\
 &\quad + \|(I + L_{\mathcal{N}}\Delta t)\delta_{n+1}^{(1)}\|_{\mathcal{N}} \|v^{n+1}\|_{\mathcal{N}} \\
 &\leq \frac{(1+\kappa)^2}{2\varepsilon^2}\Delta t \|v^n\|_{\mathcal{N}}^2 + \frac{\varepsilon^2}{2}\Delta t \|\Delta_{\mathcal{N}}v^n\|_{\mathcal{N}}^2 + \frac{\Delta t}{2\varepsilon^2}\|v^{n+1}\|_{\mathcal{N}}^2 + \frac{\varepsilon^2}{2}\Delta t \|\Delta_{\mathcal{N}}v^{n+1}\|_{\mathcal{N}}^2 \\
 &\quad + \frac{\varepsilon^2}{2\Delta t} \|(I + L_{\mathcal{N}}\Delta t)\delta_{n+1}^{(1)}\|_{\mathcal{N}}^2 + \frac{\Delta t}{2\varepsilon^2} \|v^{n+1}\|_{\mathcal{N}}^2,
 \end{aligned}$$

that is, for $0 \leq n \leq N_t - 1$,

$$\begin{aligned}
 &\frac{1}{2}(\|v^{n+1}\|_{\mathcal{N}}^2 - \|v^n\|_{\mathcal{N}}^2) + \frac{\varepsilon^2}{2}\Delta t(\|\Delta_{\mathcal{N}}v^{n+1}\|_{\mathcal{N}}^2 - \|\Delta_{\mathcal{N}}v^n\|_{\mathcal{N}}^2) \\
 &\leq \frac{\Delta t}{\varepsilon^2} \|v^{n+1}\|_{\mathcal{N}}^2 + \frac{(1+\kappa)^2}{2\varepsilon^2}\Delta t \|v^n\|_{\mathcal{N}}^2 + \frac{\varepsilon^2}{2\Delta t} \|(I + L_{\mathcal{N}}\Delta t)\delta_{n+1}^{(1)}\|_{\mathcal{N}}^2.
 \end{aligned}$$

Summing the above inequality from 0 to n leads to

$$\begin{aligned}
 &\frac{1}{2}(\|v^{n+1}\|_{\mathcal{N}}^2 - \|v^0\|_{\mathcal{N}}^2) + \frac{\varepsilon^2}{2}\Delta t(\|\Delta_{\mathcal{N}}v^{n+1}\|_{\mathcal{N}}^2 - \|\Delta_{\mathcal{N}}v^0\|_{\mathcal{N}}^2) \\
 &\leq \frac{\Delta t}{\varepsilon^2} \sum_{k=0}^n \|v^{k+1}\|_{\mathcal{N}}^2 + \frac{(1+\kappa)^2}{2\varepsilon^2}\Delta t \sum_{k=0}^n \|v^k\|_{\mathcal{N}}^2 + \frac{\varepsilon^2}{2\Delta t} \sum_{k=0}^n \|(I + L_{\mathcal{N}}\Delta t)\delta_{k+1}^{(1)}\|_{\mathcal{N}}^2 \\
 &= \frac{\Delta t}{\varepsilon^2} \|v^{n+1}\|_{\mathcal{N}}^2 + \frac{\kappa^2 + 2\kappa + 3}{2\varepsilon^2}\Delta t \sum_{k=1}^n \|v^k\|_{\mathcal{N}}^2 + \frac{\varepsilon^2}{2\Delta t} \sum_{k=0}^n \|(I + L_{\mathcal{N}}\Delta t)\delta_{k+1}^{(1)}\|_{\mathcal{N}}^2
 \end{aligned}$$

and, consequently,

$$\left(\frac{1}{2} - \frac{\Delta t}{\varepsilon^2}\right) \|v^{n+1}\|_{\mathcal{N}}^2 \leq \frac{\kappa^2 + 2\kappa + 3}{2\varepsilon^2}\Delta t \sum_{k=1}^n \|v^k\|_{\mathcal{N}}^2 + \frac{\varepsilon^2}{2\Delta t} \sum_{k=0}^n \|(I + L_{\mathcal{N}}\Delta t)\delta_{k+1}^{(1)}\|_{\mathcal{N}}^2.$$

Since $\Delta t \leq \frac{\varepsilon^2}{4}$, we have

$$\begin{aligned} \|v^{n+1}\|_{\mathcal{N}}^2 &\leq \frac{2(\kappa^2 + 2\kappa + 3)}{\varepsilon^2} \Delta t \sum_{k=1}^n \|v^k\|_{\mathcal{N}}^2 + \frac{2\varepsilon^2}{\Delta t} \cdot \frac{M_1^2}{4T} \Delta t^4 (n+1) \\ &\leq \frac{2(\kappa^2 + 2\kappa + 3)}{\varepsilon^2} \Delta t \sum_{k=1}^n \|v^k\|_{\mathcal{N}}^2 + \frac{1}{2} \varepsilon^2 M_1^2 \Delta t^2, \quad 0 \leq n \leq N_t - 1. \end{aligned}$$

An application of the discrete Gronwall inequality [5] leads to

$$\|v^{n+1}\|_{\mathcal{N}}^2 \leq \frac{1}{2} \varepsilon^2 M_1^2 e^{2(\kappa^2 + 2\kappa + 3)T/\varepsilon^2} \Delta t^2, \quad 0 \leq n \leq N_t - 1,$$

which gives us (4.5) with $C_1 = \frac{\sqrt{2}}{2} \varepsilon M_1 e^{(\kappa^2 + 2\kappa + 3)T/\varepsilon^2}$. □

The condition $u_e \in H^1(0, T; H_{\text{per}}^{m+6}(\Omega))$ implies $\Delta_{\mathcal{N}}^3 \tilde{u} \in H^1(0, T; \mathcal{M}^{\mathcal{N}})$, which leads to $(I + L_{\mathcal{N}} \Delta t) F'_{\mathcal{N}} \in L^2(0, T; \mathcal{M}^{\mathcal{N}})$ in Lemma 4.2. Therefore, the direct combination of Lemmas 4.1 and 4.2 gives us the following result on the error estimate of the ETD1 scheme.

Theorem 4.3. *Assume that $u_e \in H^1(0, T; H_{\text{per}}^{m+6}(\Omega))$ with $m \geq 2$ and $\{u^n\}_{n=1}^{N_t}$ be the approximate solution calculated by the ETD1 scheme (2.10) with $u^0 = u(0)$. If the time step size $\Delta t \leq \frac{\varepsilon^2}{4}$, then we have*

$$\|u(t_n) - u^n\|_{\mathcal{N}} \leq C(\Delta t + N^{-m}), \quad 1 \leq n \leq N_t,$$

where $C > 0$ is a constant independent on Δt and N .

Finally, we turn to the error estimates of the ETDMS2 scheme (2.11) with $u^0 = \tilde{u}(0)$ and u^1 calculated by the ETD1 scheme (2.10). Setting $n = 0$, acting as $(I + L_{\mathcal{N}} \Delta t)$ on both sides, and then taking the discrete L^2 inner product with $2v^1$ in (4.7), we first have

$$2\|v^1\|_{\mathcal{N}}^2 + 2\varepsilon^2 \Delta t \|\Delta_{\mathcal{N}} v^1\|_{\mathcal{N}}^2 + 2\kappa \Delta t \|\nabla_{\mathcal{N}} v^1\|_{\mathcal{N}}^2 \leq \|(I + L_{\mathcal{N}} \Delta t) \delta_1^{(1)}\|_{\mathcal{N}}^2 + \|v^1\|_{\mathcal{N}}^2.$$

For any $\Delta t > 0$, it holds that

$$(4.9) \quad \|v^1\|_{\mathcal{N}}^2 + 2\varepsilon^2 \Delta t \|\Delta_{\mathcal{N}} v^1\|_{\mathcal{N}}^2 \leq \frac{M_1^2}{4T} \Delta t^4.$$

Lemma 4.4. *Assume that $\{u^n\}_{n=2}^{N_t}$ is calculated by the ETDMS2 scheme (2.11) with $u^0 = \tilde{u}(0)$ and u^1 calculated by the ETD1 scheme (2.10). If $(I + L_{\mathcal{N}} \Delta t) F''_{\mathcal{N}} \in L^2(0, T; \mathcal{M}^{\mathcal{N}})$ and the time step size $\Delta t \leq \frac{\varepsilon^2}{2(\kappa^2 + 4\kappa + 5)}$, then we have*

$$(4.10) \quad \|\tilde{u}(t_n) - u^n\|_{\mathcal{N}} \leq C_2 \Delta t^2, \quad 1 \leq n \leq N_t,$$

where $C_2 > 0$ is a constant independent on Δt and N .

Proof. The space-discrete solution $\tilde{u}(t_{n+1})$ could be regarded as satisfying (2.11) with a defect $\delta_{n+1}^{(2)}$,

$$(4.11) \quad \tilde{u}(t_{n+1}) = e^{-L_{\mathcal{N}} \Delta t} \tilde{u}(t_n) - (\phi_0(L_{\mathcal{N}}) + \phi_1(L_{\mathcal{N}})) F_{\mathcal{N}}(t_n) + \phi_1(L_{\mathcal{N}}) F_{\mathcal{N}}(t_{n-1}) - \delta_{n+1}^{(2)}$$

for $1 \leq n \leq N_t - 1$ where

$$\begin{aligned} \delta_{n+1}^{(2)} &= \int_0^{\Delta t} e^{-L_{\mathcal{N}}(\Delta t - \tau)} \left(F_{\mathcal{N}}(t_n + \tau) - \left(1 + \frac{\tau}{\Delta t} \right) F_{\mathcal{N}}(t_n) + \frac{\tau}{\Delta t} F_{\mathcal{N}}(t_{n-1}) \right) d\tau \\ &= \int_0^{\Delta t} e^{-L_{\mathcal{N}}(\Delta t - \tau)} \int_0^{\tau} \int_{-\frac{\Delta t}{\tau}\sigma}^{\sigma} F''_{\mathcal{N}}(t_n + \xi) d\xi d\sigma d\tau. \end{aligned}$$

Let $M_2 = \|(I + L_{\mathcal{N}}\Delta t)F''_{\mathcal{N}}\|_{L^2(0,T;\mathcal{M}^{\mathcal{N}})}$. Since

$$\begin{aligned} &\int_0^{\tau} \int_{-\frac{\Delta t}{\tau}\sigma}^{\sigma} \|(I + L_{\mathcal{N}}\Delta t)F''_{\mathcal{N}}(t_n + \xi)\|_{\mathcal{N}} d\xi d\sigma \\ &= \frac{\tau(\tau + \Delta t)}{T^3} \int_0^T \sigma \int_0^T \left\| (I + L_{\mathcal{N}}\Delta t)F''_{\mathcal{N}}\left(t_n - \frac{\Delta t}{T}\sigma + \frac{\tau + \Delta t}{T^2}\sigma\xi\right) \right\|_{\mathcal{N}} d\xi d\sigma \\ &\leq \frac{\tau(\tau + \Delta t)}{T^3} M_2 \sqrt{T} \int_0^T \sigma d\sigma = \frac{\tau(\tau + \Delta t)}{2\sqrt{T}} M_2, \end{aligned}$$

we have

$$\begin{aligned} &\|(I + L_{\mathcal{N}}\Delta t)\delta_{n+1}^{(2)}\|_{\mathcal{N}} \\ &\leq \int_0^{\Delta t} \|e^{-L_{\mathcal{N}}(\Delta t - \tau)}\| \int_0^{\tau} \int_{-\frac{\Delta t}{\tau}\sigma}^{\sigma} \|(I + L_{\mathcal{N}}\Delta t)F''_{\mathcal{N}}(t_n + \xi)\|_{\mathcal{N}} d\xi d\sigma d\tau \\ &\leq \frac{M_2}{2\sqrt{T}} \int_0^{\Delta t} \tau(\tau + \Delta t)e^{-\lambda_{\min}(\Delta t - \tau)} d\tau \\ &= \frac{M_2}{2\sqrt{T}} \Delta t^3 \cdot \frac{1 - \lambda_{\min}\Delta t + \frac{1}{2}(\lambda_{\min}\Delta t)^2 - e^{-\lambda_{\min}\Delta t}}{(\lambda_{\min}\Delta t)^3} \leq \frac{M_2}{12\sqrt{T}} \Delta t^3. \end{aligned}$$

Let $v^n = \tilde{u}(t_n) - u^n$. The difference between (2.11) and (4.11) gives

$$\begin{aligned} (4.12) \quad v^{n+1} &= e^{-L_{\mathcal{N}}\Delta t}v^n - (\phi_0(L_{\mathcal{N}}) + \phi_1(L_{\mathcal{N}}))(f_{\mathcal{N}}(\tilde{u}(t_n)) - f_{\mathcal{N}}(u^n)) \\ &\quad + \phi_1(L_{\mathcal{N}})(f_{\mathcal{N}}(\tilde{u}(t_{n-1})) - f_{\mathcal{N}}(u^{n-1})) - \delta_{n+1}^{(2)}, \quad 1 \leq n \leq N_t - 1, \end{aligned}$$

with $v^0 = 0$ and v^1 satisfying (4.9). Acting $(I + L_{\mathcal{N}}\Delta t)$ on both sides of (4.12) and taking the discrete L^2 inner product with v^{n+1} yield

$$\|v^{n+1}\|_{\mathcal{N}}^2 + \varepsilon^2 \Delta t \|\Delta_{\mathcal{N}}v^{n+1}\|_{\mathcal{N}}^2 + \kappa \Delta t \|\nabla_{\mathcal{N}}v^{n+1}\|_{\mathcal{N}}^2 = \text{RHS}, \quad 1 \leq n \leq N_t - 1,$$

where

$$\begin{aligned} \text{RHS} &= (q_1(L_{\mathcal{N}}\Delta t)v^n - (q_2(L_{\mathcal{N}}\Delta t) + q_3(L_{\mathcal{N}}\Delta t))\Delta t(f_{\mathcal{N}}(\tilde{u}(t_n)) - f_{\mathcal{N}}(u^n)) \\ &\quad + q_3(L_{\mathcal{N}}\Delta t)\Delta t(f_{\mathcal{N}}(\tilde{u}(t_{n-1})) - f_{\mathcal{N}}(u^{n-1})) - (I + L_{\mathcal{N}}\Delta t)\delta_{n+1}^{(2)}, v^{n+1})_{\mathcal{N}} \end{aligned}$$

with q_1, q_2 defined as before and

$$q_3(a) = \frac{(1+a)(e^{-a} - 1 + a)}{a^2}.$$

Since $\frac{1}{2} < q_3(a) < 1$ for any $a > 0$, we get

$$\begin{aligned}
\text{RHS} &\leq \|q_1(L_{\mathcal{N}}\Delta t)\| \|v^n\|_{\mathcal{N}} \|v^{n+1}\|_{\mathcal{N}} \\
&\quad + (1 + \kappa)\Delta t \|q_2(L_{\mathcal{N}}\Delta t) + q_3(L_{\mathcal{N}}\Delta t)\| \|\nabla_{\mathcal{N}}v^n\|_{\mathcal{N}} \|\nabla_{\mathcal{N}}v^{n+1}\|_{\mathcal{N}} \\
&\quad + (1 + \kappa)\Delta t \|q_3(L_{\mathcal{N}}\Delta t)\| \|\nabla_{\mathcal{N}}v^{n-1}\|_{\mathcal{N}} \|\nabla_{\mathcal{N}}v^{n+1}\|_{\mathcal{N}} \\
&\quad + \|(I + L_{\mathcal{N}}\Delta t)\delta_{n+1}^{(2)}\|_{\mathcal{N}} \|v^{n+1}\|_{\mathcal{N}} \\
&\leq \|v^n\|_{\mathcal{N}} \|v^{n+1}\|_{\mathcal{N}} + 3(1 + \kappa)\Delta t \|\nabla_{\mathcal{N}}v^n\|_{\mathcal{N}} \|\nabla_{\mathcal{N}}v^{n+1}\|_{\mathcal{N}} \\
&\quad + (1 + \kappa)\Delta t \|\nabla_{\mathcal{N}}v^{n-1}\|_{\mathcal{N}} \|\nabla_{\mathcal{N}}v^{n+1}\|_{\mathcal{N}} + \|(I + L_{\mathcal{N}}\Delta t)\delta_{n+1}^{(2)}\|_{\mathcal{N}} \|v^{n+1}\|_{\mathcal{N}} \\
&\leq \frac{1}{2} \|v^n\|_{\mathcal{N}}^2 + \frac{1}{2} \|v^{n+1}\|_{\mathcal{N}}^2 + \frac{3(1 + \kappa)}{2} \Delta t \|\nabla_{\mathcal{N}}v^n\|_{\mathcal{N}}^2 + \frac{3(1 + \kappa)}{2} \Delta t \|\nabla_{\mathcal{N}}v^{n+1}\|_{\mathcal{N}}^2 \\
&\quad + \frac{1 + \kappa}{2} \Delta t \|\nabla_{\mathcal{N}}v^{n-1}\|_{\mathcal{N}}^2 + \frac{1 + \kappa}{2} \Delta t \|\nabla_{\mathcal{N}}v^{n+1}\|_{\mathcal{N}}^2 \\
&\quad + \|(I + L_{\mathcal{N}}\Delta t)\delta_{n+1}^{(2)}\|_{\mathcal{N}} \|v^{n+1}\|_{\mathcal{N}}.
\end{aligned}$$

Thus we have

$$\begin{aligned}
&\frac{1}{2} (\|v^{n+1}\|_{\mathcal{N}}^2 - \|v^n\|_{\mathcal{N}}^2) + \varepsilon^2 \Delta t \|\Delta_{\mathcal{N}}v^{n+1}\|_{\mathcal{N}}^2 \\
&\leq (2 + \kappa)\Delta t \|\nabla_{\mathcal{N}}v^{n+1}\|_{\mathcal{N}}^2 + \frac{3(1 + \kappa)}{2} \Delta t \|\nabla_{\mathcal{N}}v^n\|_{\mathcal{N}}^2 \\
&\quad + \frac{1 + \kappa}{2} \Delta t \|\nabla_{\mathcal{N}}v^{n-1}\|_{\mathcal{N}}^2 + \|(I + L_{\mathcal{N}}\Delta t)\delta_{n+1}^{(2)}\|_{\mathcal{N}} \|v^{n+1}\|_{\mathcal{N}} \\
&\leq (2 + \kappa)\Delta t \|v^{n+1}\|_{\mathcal{N}} \|\Delta_{\mathcal{N}}v^{n+1}\|_{\mathcal{N}} + \frac{3(1 + \kappa)}{2} \Delta t \|v^n\|_{\mathcal{N}} \|\Delta_{\mathcal{N}}v^n\|_{\mathcal{N}} \\
&\quad + \frac{1 + \kappa}{2} \Delta t \|v^{n-1}\|_{\mathcal{N}} \|\Delta_{\mathcal{N}}v^{n-1}\|_{\mathcal{N}} + \|(I + L_{\mathcal{N}}\Delta t)\delta_{n+1}^{(2)}\|_{\mathcal{N}} \|v^{n+1}\|_{\mathcal{N}} \\
&\leq \frac{(2 + \kappa)^2}{2\varepsilon^2} \Delta t \|v^{n+1}\|_{\mathcal{N}}^2 + \frac{\varepsilon^2}{2} \Delta t \|\Delta_{\mathcal{N}}v^{n+1}\|_{\mathcal{N}}^2 \\
&\quad + \frac{9(1 + \kappa)^2}{4\varepsilon^2} \Delta t \|v^n\|_{\mathcal{N}}^2 + \frac{\varepsilon^2}{4} \Delta t \|\Delta_{\mathcal{N}}v^n\|_{\mathcal{N}}^2 + \frac{(1 + \kappa)^2}{4\varepsilon^2} \Delta t \|v^{n-1}\|_{\mathcal{N}}^2 \\
&\quad + \frac{\varepsilon^2}{4} \Delta t \|\Delta_{\mathcal{N}}v^{n-1}\|_{\mathcal{N}}^2 + \frac{\varepsilon^2}{2\Delta t} \|(I + L_{\mathcal{N}}\Delta t)\delta_{n+1}^{(2)}\|_{\mathcal{N}}^2 + \frac{\Delta t}{2\varepsilon^2} \|v^{n+1}\|_{\mathcal{N}}^2,
\end{aligned}$$

that is, for $1 \leq n \leq N_t - 1$,

$$\begin{aligned}
&\frac{1}{2} (\|v^{n+1}\|_{\mathcal{N}}^2 - \|v^n\|_{\mathcal{N}}^2) + \frac{\varepsilon^2}{2} \Delta t (\|\Delta_{\mathcal{N}}v^{n+1}\|_{\mathcal{N}}^2 - \frac{1}{2} \|\Delta_{\mathcal{N}}v^n\|_{\mathcal{N}}^2 - \frac{1}{2} \|\Delta_{\mathcal{N}}v^{n-1}\|_{\mathcal{N}}^2) \\
&\leq \frac{\kappa^2 + 4\kappa + 5}{2\varepsilon^2} \Delta t \|v^{n+1}\|_{\mathcal{N}}^2 + \frac{9(1 + \kappa)^2}{4\varepsilon^2} \Delta t \|v^n\|_{\mathcal{N}}^2 + \frac{(1 + \kappa)^2}{4\varepsilon^2} \Delta t \|v^{n-1}\|_{\mathcal{N}}^2 \\
&\quad + \frac{\varepsilon^2}{2\Delta t} \|(I + L_{\mathcal{N}}\Delta t)\delta_{n+1}^{(2)}\|_{\mathcal{N}}^2.
\end{aligned}$$

Summing the above inequality from 1 to n leads to

$$\begin{aligned} & \frac{1}{2}(\|v^{n+1}\|_{\mathcal{N}}^2 - \|v^1\|_{\mathcal{N}}^2) \\ & + \frac{\varepsilon^2}{2}\Delta t(\|\Delta_{\mathcal{N}}v^{n+1}\|_{\mathcal{N}}^2 + \frac{1}{2}\|\Delta_{\mathcal{N}}v^n\|_{\mathcal{N}}^2 - \|\Delta_{\mathcal{N}}v^1\|_{\mathcal{N}}^2 - \frac{1}{2}\|\Delta_{\mathcal{N}}v^0\|_{\mathcal{N}}^2) \\ & \leq \frac{\kappa^2 + 4\kappa + 5}{2\varepsilon^2}\Delta t \sum_{k=1}^n \|v^{k+1}\|_{\mathcal{N}}^2 + \frac{9(1 + \kappa)^2}{4\varepsilon^2}\Delta t \sum_{k=1}^n \|v^k\|_{\mathcal{N}}^2 \\ & + \frac{(1 + \kappa)^2}{4\varepsilon^2}\Delta t \sum_{k=1}^n \|v^{k-1}\|_{\mathcal{N}}^2 + \frac{\varepsilon^2}{2\Delta t} \sum_{k=1}^n \|(I + L_{\mathcal{N}}\Delta t)\delta_{k+1}^{(2)}\|_{\mathcal{N}}^2 \\ & \leq \frac{\kappa^2 + 4\kappa + 5}{2\varepsilon^2}\Delta t\|v^{n+1}\|_{\mathcal{N}}^2 + \frac{3\kappa^2 + 7\kappa + 5}{\varepsilon^2}\Delta t \sum_{k=2}^n \|v^k\|_{\mathcal{N}}^2 \\ & + \frac{5(1 + \kappa)^2}{2\varepsilon^2}\Delta t\|v^1\|_{\mathcal{N}}^2 + \frac{\varepsilon^2}{2\Delta t} \sum_{k=1}^n \|(I + L_{\mathcal{N}}\Delta t)\delta_{k+1}^{(2)}\|_{\mathcal{N}}^2 \end{aligned}$$

and, consequently,

$$\begin{aligned} & \left(\frac{1}{2} - \frac{\kappa^2 + 4\kappa + 5}{2\varepsilon^2}\Delta t\right)\|v^{n+1}\|_{\mathcal{N}}^2 \\ & \leq \frac{3\kappa^2 + 7\kappa + 5}{\varepsilon^2}\Delta t \sum_{k=2}^n \|v^k\|_{\mathcal{N}}^2 + \left(\frac{1}{2} + \frac{5(1 + \kappa)^2}{2\varepsilon^2}\Delta t\right)\|v^1\|_{\mathcal{N}}^2 \\ & + \frac{\varepsilon^2}{2}\Delta t\|\Delta_{\mathcal{N}}v^1\|_{\mathcal{N}}^2 + \frac{\varepsilon^2}{2\Delta t} \sum_{k=1}^n \|(I + L_{\mathcal{N}}\Delta t)\delta_{k+1}^{(2)}\|_{\mathcal{N}}^2. \end{aligned}$$

Since $\Delta t \leq \frac{\varepsilon^2}{2(\kappa^2 + 4\kappa + 5)}$, we have

$$\begin{aligned} \|v^{n+1}\|_{\mathcal{N}}^2 & \leq \frac{4(3\kappa^2 + 7\kappa + 5)}{\varepsilon^2}\Delta t \sum_{k=2}^n \|v^k\|_{\mathcal{N}}^2 + \left(2 + \frac{5\kappa^2 + 10\kappa + 5}{\kappa^2 + 4\kappa + 5}\right)\|v^1\|_{\mathcal{N}}^2 \\ & + 2\varepsilon^2\Delta t\|\Delta_{\mathcal{N}}v^1\|_{\mathcal{N}}^2 + \frac{2\varepsilon^2}{\Delta t} \cdot \frac{M_2^2}{144T}\Delta t^6n \\ & \leq \frac{4(3\kappa^2 + 7\kappa + 5)}{\varepsilon^2}\Delta t \sum_{k=2}^n \|v^k\|_{\mathcal{N}}^2 + 7\|v^1\|_{\mathcal{N}}^2 + 2\varepsilon^2\Delta t\|\Delta_{\mathcal{N}}v^1\|_{\mathcal{N}}^2 + \frac{\varepsilon^2M_2^2}{72}\Delta t^4 \end{aligned}$$

for $1 \leq n \leq N_t - 1$. Combining the above inequality with (4.9), it holds that

$$\|v^{n+1}\|_{\mathcal{N}}^2 \leq \frac{4(3\kappa^2 + 7\kappa + 5)}{\varepsilon^2}\Delta t \sum_{k=2}^n \|v^k\|_{\mathcal{N}}^2 + \left(\frac{7M_1^2}{4T} + \frac{\varepsilon^2M_2^2}{72}\right)\Delta t^4, \quad 1 \leq n \leq N_t - 1.$$

Using the discrete Gronwall inequality, we finally obtain

$$\|v^{n+1}\|_{\mathcal{N}}^2 \leq \left(\frac{7M_1^2}{4T} + \frac{\varepsilon^2M_2^2}{72}\right)e^{4(3\kappa^2 + 7\kappa + 5)T/\varepsilon^2}\Delta t^4, \quad 1 \leq n \leq N_t - 1.$$

Combining with (4.9), we obtain (4.10) with $C_2 = \sqrt{\frac{7M_1^2}{4T} + \frac{\varepsilon^2M_2^2}{72}}e^{2(3\kappa^2 + 7\kappa + 5)T/\varepsilon^2}$. □

Noticing that $u_e \in H^2(0, T; H_{\text{per}}^{m+6}(\Omega))$ implies $(I + L_N \Delta t) F_N'' \in L^2(0, T; \mathcal{M}^N)$ in Lemma 4.4, thus the combination of Lemmas 4.1 and 4.4 gives us the following result on the error estimate of the ETDMs2 scheme.

Theorem 4.5. *Assume that $u_e \in H^2(0, T; H_{\text{per}}^{m+6}(\Omega))$ with $m \geq 2$ and $\{u^n\}_{n=2}^{N_t}$ is the approximate solution calculated by the ETDMs2 scheme (2.11) with $u^0 = u(0)$ and u^1 being calculated by the ETD1 scheme (2.10). If the time step size $\Delta t \leq \frac{\varepsilon^2}{2(\kappa^2 + 4\kappa + 5)}$, then we have*

$$\|u(t_n) - u^n\|_N \leq C(\Delta t^2 + N^{-m}), \quad 1 \leq n \leq N_t,$$

where $C > 0$ is a constant independent on Δt and N .

Remark 4.6. We have seen from Theorems 4.3 and 4.5 that there exists a constraint taking the form $\Delta t \leq C\varepsilon^2$ for the convergence. Actually, such constraints on the time step size are not excessive since they are necessary to prove the convergence of all the similar numerical schemes for the model (1.1); see, e.g., [22, 30].

5. NUMERICAL EXPERIMENTS

In this section, we carry out various numerical experiments to verify the temporal convergence rates of the ETD1 and ETDMs2 schemes, and to simulate the coarsening dynamics of the epitaxial thin film growth by using the ETDMs2 scheme. We set $\kappa = \frac{1}{8}$ in all experiments.

5.1. Convergence tests. We considered the evolutions governed by the equation (1.1) with $\varepsilon^2 = 0.1$ on the domain $\Omega = (0, 2\pi) \times (0, 2\pi)$ up to the time $T = 0.05$. The initial condition was set to be $u_0(x, y) = 0.1(\sin 3x \sin 2y + \sin 5x \sin 5y)$ on the uniform mesh with $N_x = N_y = N$.

First, we conducted experiments to verify the spatial spectral accuracy. To eliminate the time-marching effect, we adopted the ETD1 scheme (2.10) with $\Delta t = T$; in other words, we only considered the convergence of the Fourier collocation approximation applied on the periodic boundary-value problem of an ellipse equation. We interpolated the grid function $u^N \in \mathcal{M}^N$ by

$$U_N(x, y) = \sum_{k, l = -\frac{N}{2}}^{\frac{N}{2}} \frac{\hat{u}_{kl}^N}{c_k c_l} \exp\{i(kx + ly)\}, \quad (x, y) \in \Omega,$$

where $c_p = 2$ for $|p| = \frac{N}{2}$ and $c_p = 1$ for $|p| < \frac{N}{2}$, and

$$\hat{u}_{kl}^N = \frac{1}{N^2} \sum_{i, j=1}^N u_{ij}^N \exp\{-i(kx_i + ly_j)\}, \quad -\frac{N}{2} \leq k, l \leq \frac{N}{2}.$$

We took the interpolation U_N with $N = 2048$ as the benchmark solution and defined the L^2 errors as

$$\text{err}(N) = \frac{2\pi}{N} \sqrt{\sum_{i, j=1}^N |u_{ij}^N - U_{2048}(x_i, y_j)|^2}.$$

The values $\text{err}(N)$ with $N = 8k$, $k = 1, 2, \dots, 37$ are shown in Figure 1 where the spectral accuracy is obvious.

Second, we tested the convergence rates in time of the ETD1 and ETDMs2 schemes. For the purpose of comparison, we also computed numerical errors of

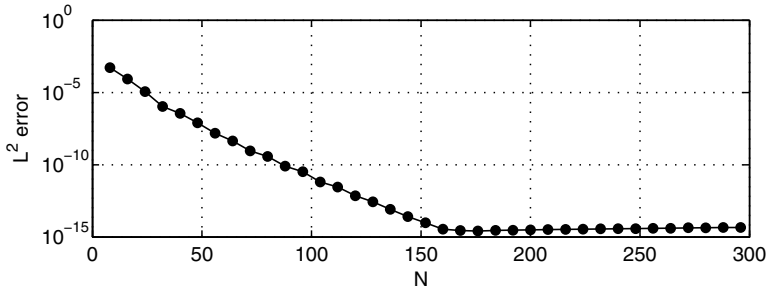


FIGURE 1. Spectral accuracy in space for the ETD1 scheme (2.10).

the SSI1 scheme. We fixed $N = 1024$ and performed the numerical simulations up to the time $T = 10\delta$ using the time step sizes $\Delta t = 2^{-k}\delta$, $k = 0, 1, 2, \dots, 8$ with $\delta = 0.005$. The approximate solution obtained by using the ETDMs2 scheme with $\Delta t = 2^{-8}\delta/5$ was taken as the benchmark solution for calculating errors. The discrete L^2 -errors of the numerical solutions are shown in Figure 2(a) where the first order accuracy of the SSI1 and ETD1 schemes and the second order accuracy of the ETDMs2 scheme are seen obviously. In addition, the errors of the ETD1 scheme are smaller than those of the SSI1 scheme although they have the same order of convergence. For a given level of accuracy, for example, 10^{-5} , we found that the time consumption of the SSI1 scheme is about four times as much as the ETD1 scheme and nearly a hundred times as much as the ETDMs2 scheme.

We also repeated the above experiments using $\varepsilon^2 = 0.01$. It is easy to find from Figure 2(b) that smaller ε leads to larger errors while the convergence rates are independent on the value of ε .

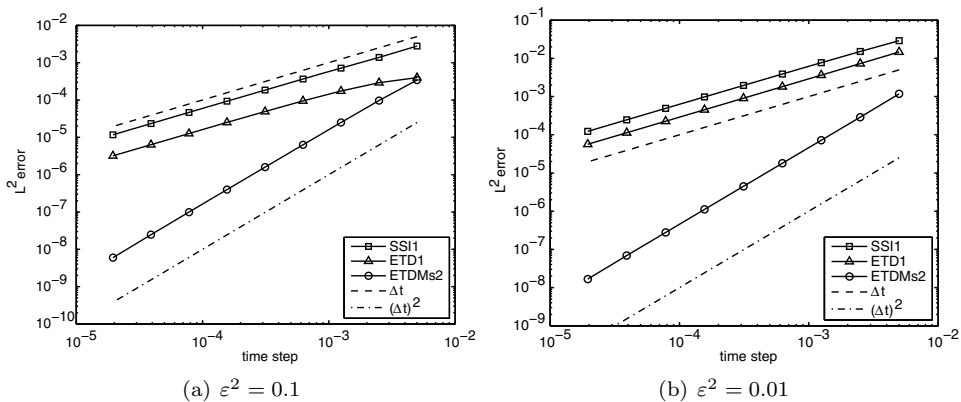


FIGURE 2. Convergence rates in time of the SSI1, ETD1, and ETDMs2 schemes.

5.2. Coarsening dynamics. To observe the longtime behaviors of the thin film growth, such as the energy decay rate and the surface roughness growth rate, we simulated the equation (1.1) with the parameters $\varepsilon = 0.1, 0.09, \dots, 0.01$ by using the ETDMs2 scheme (2.11). We took a large domain $\Omega = (0, 12.8) \times (0, 12.8)$ and

used the uniform mesh with $N_x = N_y = N$. The initial condition was set to be a random state given by random numbers varying uniformly from -0.001 to 0.001 on each grid points. We used $N = 512$ for $\varepsilon \geq 0.03$, $N = 1024$ for $\varepsilon = 0.02$, and $N = 2048$ for $\varepsilon = 0.01$. For the time step sizes, we set $\Delta t = 0.001$ on the time interval $[0, 400)$, $\Delta t = 0.01$ on the time interval $[400, 6000)$, $\Delta t = 0.1$ on the time interval $[6000, 100000]$, and $\Delta t = 0.5$ for $t > 100000$ if needed.

Figure 3 shows the time snapshots of the calculated height u with $\varepsilon = 0.01$. Coarsening dynamics with shapes of hills and valleys in the system is evident. At the early period, there are many small hills (red part) and valleys (blue part), while at the final time $t = 2 \times 10^6$, the system saturates to a one-hill-one-valley structure.

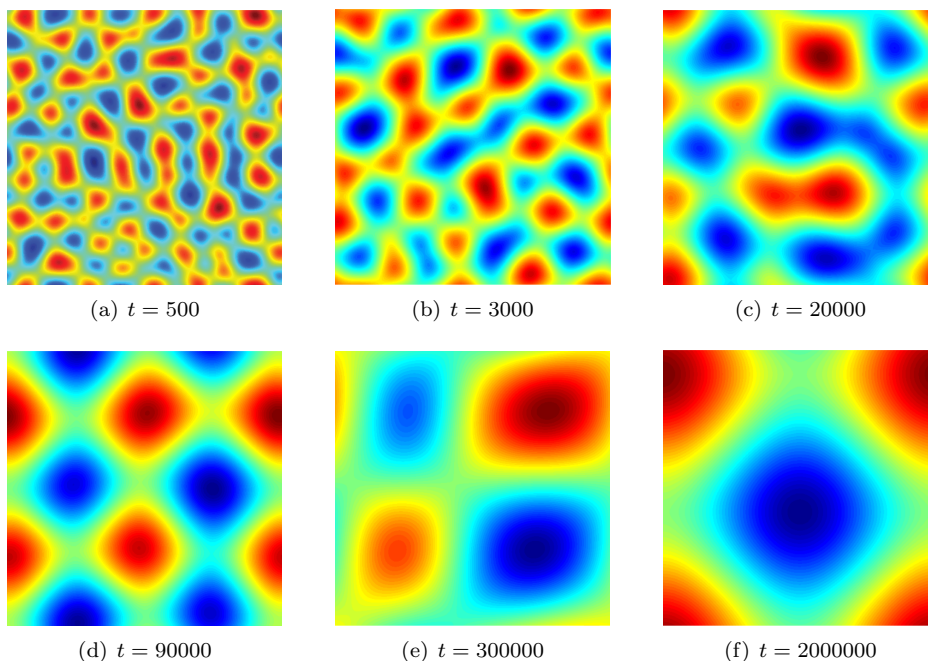


FIGURE 3. Time snapshots of the calculated height u with $\varepsilon = 0.01$.

The energy $E(t)$ is defined in (1.3), the surface roughness $R(t)$ and the mound width $W(t)$ are defined as

$$R(t) = \sqrt{\frac{1}{|\Omega|} \int_{\Omega} |u(\mathbf{x}, t) - \bar{u}(t)|^2 d\mathbf{x}}, \quad W(t) = \sqrt{\frac{1}{|\Omega|} \int_{\Omega} |\nabla u(\mathbf{x}, t)|^2 d\mathbf{x}}$$

with $\bar{u}(t) = \frac{1}{|\Omega|} \int_{\Omega} u(\mathbf{x}, t) d\mathbf{x}$. For the no-slope-selection epitaxial growth model (1.1), it is shown in [11, 18] that

$$E(t) \sim \mathcal{O}(-\ln t), \quad R(t) \sim \mathcal{O}(t^{1/2}), \quad W(t) \sim \mathcal{O}(t^{1/4}).$$

We numerically verified these scaling laws.

Figure 4 presents the linear fitting lines for the case $\varepsilon = 0.01$. Figure 4(a) shows the linear fitting of the semi-log energy data up to $t = 6000$, where the fitting line

is of the form $E = m_e \ln t + b_e$ with $m_e = -40.719$ and $b_e = -204.967$. Figure 4(b) shows the linear fitting of the log-log surface roughness data up to $t = 6000$, where the fitting line is of the form $R = b_r t^{m_r}$ with $m_r = 0.503$ and $b_r = 0.406$. Figure 4(c) shows the linear fitting of the log-log mound width data up to $t = 6000$, where the fitting line is of the form $W = b_w t^{m_w}$ with $m_w = 0.253$ and $b_w = 5.974$. It is quite evident that the $-\ln t$, $t^{1/2}$ and $t^{1/4}$ scaling laws for the energy decay rate, the surface roughness growth rate and the mound width growth rate, respectively, are presented by our numerical simulations.

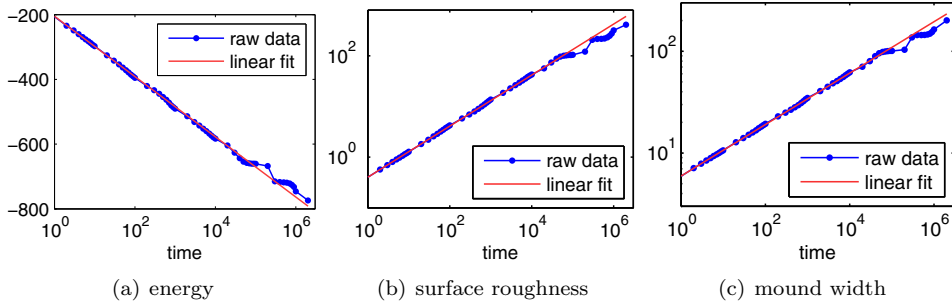


FIGURE 4. Evolutions of energy, roughness and width with $\varepsilon = 0.01$.

Table 1 gives the linear fitting coefficients $m_e, b_e, m_r, b_r, m_w, b_w$, in the same sense as above, for the cases from $\varepsilon = 0.1$ to $\varepsilon = 0.01$. We observe from Table 1 that as ε decreases, m_r and m_w approach $1/2$ and $1/4$, respectively.

TABLE 1. Coefficients of the linear fittings using data up to $t = 400$.

ε	0.1	0.09	0.08	0.07	0.06	0.05	0.04	0.03	0.02	0.01
m_e	-37.555	-38.699	-39.614	-38.294	-38.275	-39.339	-39.499	-40.038	-40.340	-40.433
b_e	-31.802	-36.781	-45.036	-57.440	-69.293	-78.960	-96.469	-119.664	-150.406	-205.071
m_r	0.548	0.550	0.548	0.526	0.520	0.523	0.516	0.513	0.510	0.504
b_r	0.315	0.320	0.334	0.354	0.366	0.359	0.373	0.388	0.394	0.401
m_w	0.289	0.289	0.285	0.273	0.268	0.269	0.264	0.261	0.258	0.253
b_w	1.548	1.660	1.819	2.016	2.232	2.444	2.804	3.323	4.125	5.947

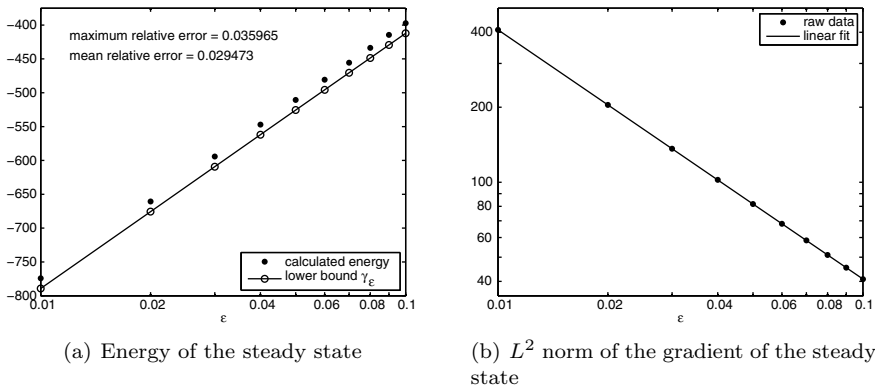
Finally, we consider the energy and L^2 norm of the gradient of the steady states for various ε values. Theoretically, the energy $E(t)$ has a lower bound [2]:

$$E(t) \geq \gamma_\varepsilon = \frac{L^2}{2} \left(\ln \frac{4\varepsilon^2 \pi^2}{L^2} - \frac{4\varepsilon^2 \pi^2}{L^2} + 1 \right).$$

Although the bound γ_ε is not sharp, the minimum calculated energies m_ε for various ε match γ_ε with about 3% accuracy; see Figure 5(a). Besides, the L^2 norm of the gradient of the steady state scales as $\mathcal{O}(1/\varepsilon)$ [18], which is also observed in our simulation, see Figure 5(b), where the fitting line is of the form $b_g \varepsilon^{m_g}$ with $m_g = -1.008$ and $b_g = 4.0782$.

6. CONCLUSIONS

In this paper, a class of exponential time differencing multistep schemes with Fourier spectral collocation for spatial discretization are presented for solving the no-slope-selection epitaxial growth model with periodic boundary condition in a

FIGURE 5. Energy and gradient of steady state versus ε .

rectangular domain. In particular, an optimal form of linear convex splitting is developed and used in the schemes for the purpose of stabilization. The first and second order schemes are theoretically and numerically proven to be energy stable with expected convergence rates. The simulated coarsening rates of the decay of energy, the growth of surface roughness and mound width are in excellent agreement with the theoretical results. We also note the analysis techniques presented in this paper can be further generalized and used to even higher order ETD schemes.

If the time integration is approximated via the interpolation of the nonlinear term instead of the extrapolation, one can similarly derive the Runge-Kutta type ETD schemes [16, 34], which may cost more calculations per time step when higher order schemes are adopted. However, the computations in each time step are independent of the results from previous time steps, which is more convenient to be used in adaptive time-stepping algorithms. Correspondingly, energy stability and convergence analysis for the ETDRK schemes could be similarly conducted. Although Fourier spectral method is used and studied for spatial discretization in this paper due to the periodic boundary condition, other spectral methods or finite difference schemes also could be used in case of the Dirichlet or Neumann boundary conditions (see, e.g., [15]). In the end, application of the ETD method to other phase field models will also be among our future works.

ACKNOWLEDGMENTS

We would like to express our deep thanks to the anonymous reviewers whose valuable suggestions helped us to improve this article greatly. We are grateful to Professor Haiwei Sun of University of Macau for many valuable comments.

REFERENCES

- [1] G. Beylkin, J. M. Keiser, and L. Vozovoi, *A new class of time discretization schemes for the solution of nonlinear PDEs*, J. Comput. Phys. **147** (1998), no. 2, 362–387, DOI 10.1006/jcph.1998.6093. MR1663563
- [2] W. Chen, S. Conde, C. Wang, X. Wang, and S. M. Wise, *A linear energy stable scheme for a thin film model without slope selection*, J. Sci. Comput. **52** (2012), no. 3, 546–562, DOI 10.1007/s10915-011-9559-2. MR2948706

- [3] W. B. Chen, C. Wang, X. M. Wang, and S. M. Wise, *A linear iteration algorithm for energy stable second order scheme for a thin film model without slope selection*, J. Sci. Comput., 59 (2014), pp. 574–601.
- [4] S. M. Cox and P. C. Matthews, *Exponential time differencing for stiff systems*, J. Comput. Phys. **176** (2002), no. 2, 430–455, DOI 10.1006/jcph.2002.6995. MR1894772
- [5] J. Dixon and S. McKee, *Weakly singular discrete Gronwall inequalities*, Z. Angew. Math. Mech. **66** (1986), no. 11, 535–544, DOI 10.1002/zamm.19860661107. MR880357
- [6] Q. Du and R. A. Nicolaides, *Numerical analysis of a continuum model of phase transition*, SIAM J. Numer. Anal. **28** (1991), no. 5, 1310–1322, DOI 10.1137/0728069. MR1119272
- [7] Q. Du and W.-x. Zhu, *Stability analysis and application of the exponential time differencing schemes*, J. Comput. Math. **22** (2004), no. 2, 200–209. MR2058932
- [8] Q. Du and W. Zhu, *Analysis and applications of the exponential time differencing schemes and their contour integration modifications*, BIT **45** (2005), no. 2, 307–328, DOI 10.1007/s10543-005-7141-8. MR2176196
- [9] D. J. Eyre, *Unconditionally gradient stable time marching the Cahn-Hilliard equation*, Computational and mathematical models of microstructural evolution (San Francisco, CA, 1998), Mater. Res. Soc. Sympos. Proc., vol. 529, MRS, Warrendale, PA, 1998, pp. 39–46, DOI 10.1557/PROC-529-39. MR1676409
- [10] D. Furihata, *A stable and conservative finite difference scheme for the Cahn-Hilliard equation*, Numer. Math. **87** (2001), no. 4, 675–699, DOI 10.1007/PL00005429. MR1815731
- [11] L. Golubović, *Interfacial coarsening in epitaxial growth models without slope selection*, Phys. Rev. Lett., 78 (1997), pp. 90–93.
- [12] N. J. Higham, *Functions of Matrices*, Society for Industrial and Applied Mathematics (SIAM), Philadelphia, PA, 2008. Theory and computation. MR2396439
- [13] M. Hochbruck and A. Ostermann, *Exponential integrators*, Acta Numer. **19** (2010), 209–286, DOI 10.1017/S0962492910000048. MR2652783
- [14] L. Ju, J. Zhang, and Q. Du, *Fast and accurate algorithms for simulating coarsening dynamics of Cahn-Hilliard equations*, Comput. Mater. Sci., 108 (2015), pp. 272–282.
- [15] L. Ju, J. Zhang, L. Zhu, and Q. Du, *Fast explicit integration factor methods for semilinear parabolic equations*, J. Sci. Comput. **62** (2015), no. 2, 431–455, DOI 10.1007/s10915-014-9862-9. MR3299200
- [16] A.-K. Kassam and L. N. Trefethen, *Fourth-order time-stepping for stiff PDEs*, SIAM J. Sci. Comput. **26** (2005), no. 4, 1214–1233, DOI 10.1137/S1064827502410633. MR2143482
- [17] B. Li and J.-G. Liu, *Thin film epitaxy with or without slope selection*, European J. Appl. Math. **14** (2003), no. 6, 713–743, DOI 10.1017/S095679250300528X. MR2034852
- [18] B. Li and J.-G. Liu, *Epitaxial growth without slope selection: energetics, coarsening, and dynamic scaling*, J. Nonlinear Sci. **14** (2004), no. 5, 429–451 (2005), DOI 10.1007/s00332-004-0634-9. MR2126166
- [19] D. Li, Z. Qiao, and T. Tang, *Characterizing the stabilization size for semi-implicit Fourier-spectral method to phase field equations*, SIAM J. Numer. Anal. **54** (2016), no. 3, 1653–1681, DOI 10.1137/140993193. MR3507555
- [20] X. Li, Z. Qiao, and H. Zhang, *An unconditionally energy stable finite difference scheme for a stochastic Cahn-Hilliard equation*, Sci. China Math. **59** (2016), no. 9, 1815–1834, DOI 10.1007/s11425-016-5137-2. MR3536036
- [21] Z. Qiao and S. Sun, *Two-phase fluid simulation using a diffuse interface model with Peng-Robinson equation of state*, SIAM J. Sci. Comput. **36** (2014), no. 4, B708–B728, DOI 10.1137/130933745. MR3246906
- [22] Z. Qiao, Z.-Z. Sun, and Z. Zhang, *Stability and convergence of second-order schemes for the nonlinear epitaxial growth model without slope selection*, Math. Comp. **84** (2015), no. 292, 653–674, DOI 10.1090/S0025-5718-2014-02874-3. MR3290959
- [23] Z. Qiao, T. Tang, and H. Xie, *Error analysis of a mixed finite element method for the molecular beam epitaxy model*, SIAM J. Numer. Anal. **53** (2015), no. 1, 184–205, DOI 10.1137/120902410. MR3296620
- [24] Z. Qiao, Z. Zhang, and T. Tang, *An adaptive time-stepping strategy for the molecular beam epitaxy models*, SIAM J. Sci. Comput. **33** (2011), no. 3, 1395–1414, DOI 10.1137/100812781. MR2813245
- [25] L. Ratke and P. W. Voorhees, *Growth and Coarsening*, Springer-Verlag, Berlin, 2002.

- [26] J. Shen, T. Tang, and L.-L. Wang, *Spectral Methods: Algorithms, Analysis and Applications*, Springer Series in Computational Mathematics, vol. 41, Springer, Heidelberg, 2011. MR2867779
- [27] J. Shen, C. Wang, X. Wang, and S. M. Wise, *Second-order convex splitting schemes for gradient flows with Ehrlich-Schwoebel type energy: application to thin film epitaxy*, SIAM J. Numer. Anal. **50** (2012), no. 1, 105–125, DOI 10.1137/110822839. MR2888306
- [28] J. Shen and X. Yang, *Numerical approximations of Allen-Cahn and Cahn-Hilliard equations*, Discrete Contin. Dyn. Syst. **28** (2010), no. 4, 1669–1691, DOI 10.3934/dcds.2010.28.1669. MR2679727
- [29] L. N. Trefethen, *Spectral methods in MATLAB*, Software, Environments, and Tools, vol. 10, Society for Industrial and Applied Mathematics (SIAM), Philadelphia, PA, 2000. MR1776072
- [30] C. Wang, X. Wang, and S. M. Wise, *Unconditionally stable schemes for equations of thin film epitaxy*, Discrete Contin. Dyn. Syst. **28** (2010), no. 1, 405–423, DOI 10.3934/dcds.2010.28.405. MR2629487
- [31] S. M. Wise, C. Wang, and J. S. Lowengrub, *An energy-stable and convergent finite-difference scheme for the phase field crystal equation*, SIAM J. Numer. Anal. **47** (2009), no. 3, 2269–2288, DOI 10.1137/080738143. MR2519603
- [32] C. Xu and T. Tang, *Stability analysis of large time-stepping methods for epitaxial growth models*, SIAM J. Numer. Anal. **44** (2006), no. 4, 1759–1779, DOI 10.1137/050628143. MR2257126
- [33] S. Zhang and M. Wang, *A nonconforming finite element method for the Cahn-Hilliard equation*, J. Comput. Phys. **229** (2010), no. 19, 7361–7372, DOI 10.1016/j.jcp.2010.06.020. MR2677783
- [34] L. Zhu, L. Ju, and W. Zhao, *Fast high-order compact exponential time differencing Runge-Kutta methods for second-order semilinear parabolic equations*, J. Sci. Comput. **67** (2016), no. 3, 1043–1065, DOI 10.1007/s10915-015-0117-1. MR3493494

DEPARTMENT OF MATHEMATICS, UNIVERSITY OF SOUTH CAROLINA, COLUMBIA, SOUTH CAROLINA 29208

E-mail address: ju@math.sc.edu

APPLIED AND COMPUTATIONAL MATHEMATICS DIVISION, BEIJING COMPUTATIONAL SCIENCE RESEARCH CENTER, BEIJING, 100193, PEOPLE'S REPUBLIC OF CHINA

E-mail address: xiaoli@csrc.ac.cn

DEPARTMENT OF APPLIED MATHEMATICS, THE HONG KONG POLYTECHNIC UNIVERSITY, HUNG HOM, KOWLOON, HONG KONG

E-mail address: zhonghua.qiao@polyu.edu.hk

LABORATORY OF MATHEMATICS AND COMPLEX SYSTEMS, MINISTRY OF EDUCATION AND SCHOOL OF MATHEMATICAL SCIENCES, BEIJING NORMAL UNIVERSITY, BEIJING, 100875, PEOPLE'S REPUBLIC OF CHINA

E-mail address: hzhang@bnu.edu.cn